NUMERICAL MODELING OF ASPHALT CRACK RESISTANCE

Enad Mahmoud, Ph.D. P.E
Imad Abdallah, Ph.D.
David Renteria, BSc.
Roberto Yanez, BSc.
Soheil Nazarian, Ph.D., P.E.

SPTC14.1-47-F

DISCLAIMER

The contents of this report reflect the views of the authors, who are responsible for the facts and accuracy of the information presented herein. This document is disseminated under the sponsorship of the Department of Transportation University Transportation Centers Program, in the interest of information exchange. The U.S. Government assumes no liability for the contents or use thereof.

TECHNICAL REPORT DOCUMENTATION PAGE

1. REPORT NO. SPTC14.1-47-F	2. GOVERNMENT ACCESSION NO.	3. RECIPIENTS CATALOG NO.
4. TITLE AND SUBTITLE NUMERICAL MODELING OF ASPHALT CRACK RESISTANCE		5. REPORT DATE October 30, 2019
		6. PERFORMING ORGANIZATION CODE
7. AUTHOR(S) Enad Mahmoud, Ph.D. P.E Imad Abdallah, Ph.D. David Renteria, BSc. Roberto Yanez, BSc. Soheil Nazarian, Ph.D., P.E.		8. PERFORMING ORGANIZATION REPORT
9. PERFORMING ORGANIZATION NAME AND ADDRESS University of Texas at El Paso 500 W University Ave, El Paso, TX 79968		10. WORK UNIT NO.
		11. CONTRACT OR GRANT NO. DTRT13-G-UTC36
12. SPONSORING AGENCY NAME AND ADDRESS Southern Plains Transportation Center 201 Stephenson Pkwy, Suite 4200 The University of Oklahoma Norman, OK 73019		13. TYPE OF REPORT AND PERIOD COVERED Final March 2015 – May 2019
		14. SPONSORING AGENCY CODE
15. SUPPLEMENTARY NOTES University Transportation Center		

16. ABSTRACT

A numerical model of the Overlay Tester (OT) and Semi-Bending Circular (SCB) test were developed. The developed models combined DEM with imaging techniques to study asphalt mix crack resistance. The materials and mixes selected covered wide range of aggregate gradations, strength, and shape properties, the mixes included were: Superpave-C, CMHB-C, and PFC, while the aggregates were: a hard limestone, soft limestone, and granite. Split tensile testing results for the nine combinations of mixes and aggregates were available in addition to the modulus, compressive strength, and split tensile for the aggregates. Results clearly indicate that the heterogonous OT-DEM model has a much better potential than the homogenous model. Further analysis indicated that the use of rigid walls to simulate the loading plates improved the simulation results. Finally, heterogeneous SCB-DEM simulations were conducted for all three mixes with three notch sizes (25.4 mm, 31.75 mm, and 38.1 mm), the numerical simulations were reliable for Superpave and CMHB mixes, the test is not recommended for mixes with high air void content, which manifest itself in this model as very weak mastic (very low bond strength), such as PFC.

17. KEY WORDS Numerical modeling, overlay tester, semi-bending circular, asphalt, crack resistant		18. DISTRIBUTION STATEMENT No restrictions. This publication is available at www.sptc.org and from the NTIS.	
19. SECURITY CLASSIF. (OF THIS REPORT) Unclassified	20. SECURITY CLASSIF. (OF THIS PAGE) Unclassified	21. NO. OF PAGES 54 + cover	22. PRICE

Metric Conversion Page

SI* (MODERN METRIC) CONVERSION FACTORS

APPROXIMATE CONVERSIONS TO SI UNITS

SYMBOL	WHEN YOU KNOW	MULTIPLY BY	TO FIND	SYMBOL
LENGTH				
in	inches	25.4	millimeters	mm
ft	feet	0.305	meters	m
yd	yards	0.914	meters	m
mi	miles	1.61	kilometers	km
AREA				
in^2	square inches	645.2	square millimeters	mm^2
ft^2	square feet	0.093	square meters	m^2
yd^2	square yard	0.836	square meters	m^2
ac	acres	0.405	hectares	ha
mi^2	square miles	2.59	square kilometers	km^2
VOLUME				
fl	fluid ounces	29.57	milliliters	m
oz	gallons	3.785	liters	L
gal	cubic feet	0.028	cubic meters	L
ft^3	cubic yards	0.765	cubic	m^3
MASS				
oz	ounces	28.35	grams	g
lb	pounds	0.454	kilograms	kg
T	short tons (2000 lb)	0.907	megagrams (or "metric ton")	Mg (or "t")
TEMPERATURE (exact degrees)				
^oF	Fahrenheit	5	(F-32)/9	^oC
			Celsius or (F-32)/1.8	
ILLUMINATION				
fc	foot-candles	10.76	lux	lx
fl	foot-Lamberts	3.426	$candela/m^2$	cd/m^2
FORCE and PRESSURE or STRESS				
lbf	poundforce	4.45	newtons	N
lbf/in^2	poundforce per square inch	6.89	kilopascals	kPa

APPROXIMATE CONVERSIONS FROM SI UNITS

SYMBOL	WHEN YOU KNOW	MULTIPLY BY	TO FIND	SYMBOL
LENGTH				
mm	millimeters	0.039	inches	in
m	meters	3.28	feet	ft
m	meters	1.09	yards	yd
km	kilometers	0.621	miles	mi
AREA				
mm^2	square millimeters	0.0016	square inches	in^2
m^2	square meters	10.764	square feet	ft^2
m^2	square meters	1.195	square yards	yd^2
ha	hectares	2.47	acres	ac
km^2	square kilometers	0.386	square miles	mi^2
VOLUME				
mL	milliliters	0.034	fluid ounces	fl oz
L	liters	0.264	gallons	gal
m^3	cubic meters	35.314	cubic feet	ft^3
m^3	cubic meters	1.307	cubic yards	yd^3
MASS				
g	grams	0.035	ounces	oz
kg	kilograms	2.202	pounds	lb
Mg (or "t")	megagrams (or "metric ton")	1.103	short tons (2000 lb)	T
TEMPERATURE (exact degrees)				
^oC	Celsius	1.8C+32	Fahrenheit	^oF
ILLUMINATION				
lx	lux	0.0929	foot-candles	fc
cd/m^2	$candela/m^2$	0.2919	foot-Lamberts	fl
FORCE and PRESSURE or STRESS				
N	newtons	0.225	poundforce	lbf
kPa	kilopascals	0.145	poundforce per square h	lbf/in^2

*SI is the symbol for the International System of Units. Appropriate rounding should be made to comply with Section 4 of ASTM E380. (Revised March 2003)

NUMERICAL MODELING OF
ASPHALT CRACK RESISTANCE

Final Report

October 2019

Enad Mahmoud, Ph.D. P.E
Imad Abdallah, Ph.D.
David Renteria, BSc.
Roberto Yanez, BSc.
Soheil Nazarian, Ph.D., P.E.

Southern Plains Transportation Center
201 Stephenson Pkwy, Suite 4200
The University of Oklahoma
Norman, OK 73019

Table of Contents

List of Figures

List of Tables

Executive Summary

A numerical model of the Overlay Tester (OT) and Semi-Bending Circular (SCB) test were developed. The developed models combined DEM with imaging techniques to study asphalt mix crack resistance. The materials and mixes selected covered wide range of aggregate gradations, strength, and shape properties, the mixes included were: Superpave-C, CMHB-C, and PFC, while the aggregates were: a hard limestone, soft limestone, and granite. Split tensile testing results for the nine combinations of mixes and aggregates were available in addition to the modulus, compressive strength, and split tensile for the aggregates. The OT model focused on damage induced in the sample within the first two loading cycle in comparison to the monotonic loading case. Homogenous samples analyses based on the tracking the number of broken bonds (cracks) within OT sample. This analysis indicated that for all the nine combinations of mixes and aggregates, more than 95% damage occurred by the end of the first cycle, which made it impossible to distinguish between asphalt mixes. Heterogeneous OT-DEM simulations for two mixes were performed and compared with the homogenous cases. The results indicated much less damage after the first loading cycle. The granite-PFC mix had 69.5% damage after the first cycle for the heterogonous case compared to 97.6% for the homogenous case, while the hard limestone-PFC mix had 79.1% damage for the heterogonous case compared to a 99.0% for the homogenous case. These results clearly indicate that the heterogonous OT-DEM model has a much better potential than the homogenous model. Further analysis indicated that the use of rigid walls to simulate the loading plates improved the simulation results. Finally, heterogeneous SCB-DEM simulations were conducted for all three mixes with three notch sizes (25.4 mm, 31.75 mm, and 38.1 mm), the numerical simulations were reliable for Superpave and CMHB mixes, the test is not recommended for mixes with high air void content, which manifest itself in this model as very weak mastic (very low bond strength), such as PFC.

Introduction

Over the past few decades, most of the state DOT's, especially in the southern region, have used stiffer hot mix asphalt (HMA) to mitigate rutting. The shift toward stiffer mixes has resulted in asphalt pavements that are more prone to reflective and fatigue cracking. Cracking in HMA usually results in much faster deterioration rates of the pavement. The Overlay Tester (OT) has been implemented by Texas Department of Transportation (TxDOT) to predict HMA resistance to cracking. However, most of the research related to OT test has focused on its variability and correlations with the field performance. Numerical simulations of the test are limited to studying the levels of stress and strain developed within the tested specimens. A numerical approach that is capable of studying the interrelated effects of aggregate strength, gradation, shape, and asphalt grade on the asphalt mix crack resistance is needed. Such approach will allow for a reduction in experimental testing and serve as a screening method prior to starting a full scale experimental testing program. It is anticipated that this approach will be beneficial to the state DOT's in general, and more specifically to the southern plains region.

Background

The background section is divided into two sub-sections to cover the literature on the two main subjects related to this proposed study: discrete element modeling and overlay tester.

Discrete Element Modeling (DEM)

DEM is a finite difference scheme used to study the interaction among assemblies of discrete elements. DEM was introduced by Cundall (1971). Cundall and Strack (1979) used this method for the simulation of two-dimensional discrete materials. The DEM concept is simple in principle since it is based on successively solving the law of motion (Newton's second law) and the force-displacement law for each element. Several research studies have successfully utilized DEM to characterize asphalt mixes and viscoelastic materials. You and Buttlar (2004) used DEM to predict the modulus of asphalt concrete mixtures across a range of loading frequencies and test temperatures

in both extension and compression. Hollow cylinder tensile test of asphalt mixes was also simulated with DEM (You and Buttlar, 2005). Abbas et al. (2005) used DEM to determine asphalt mastic stiffness by simulating mastic measurements acquired using the DSR. Abbas et al. (2007) used DEM to predict the asphalt mixture response under sinusoidal loading similar to laboratory measurements of the dynamic modulus of asphalt mixtures. Mahmoud et al. (2010a and 2010b) utilized DEM to study the influence of aggregate properties and internal structure on fracture in asphalt mixes and to evaluate the aggregate blending in asphalt mixes. Other examples of DEM research to study asphalt mixes include Dai and You (2007), Kim et al. (2008), Collop et al. (2007), Wu et al. (2011), Cai et al. (2013) and Cai et al. (2014). Liu et al. (2009), You et al. (2011); Liu and You (2011a and 2011b) illustrated the versatility and sufficiency of DEM to simulate viscoelastic behavior of asphalt materials using the Burger model. They successfully implemented viscoelastic DEM models for asphalt mixes under cyclic loading and creep compliance testing. Furthermore, they successfully studied the impact of aggregate orientation and shape properties on the idealized behaviors of asphalt mixes.

In DEM two elements are in contact if the distance between their centers is equal to or less than the summation of their radii. The contact behavior is described using up to three models: slip, stiffness, and bonding. The slip model allows slipping to occur between discrete elements by limiting the shear force. The input parameter for this model is the friction coefficient (μ). The maximum allowable contact shear force is equal to the coefficient of friction multiplied by the normal force at that contact. The stiffness model relates the contact forces and relative displacement in the normal and shear directions (normal and shear stiffness). The bonding model is a strength parameter above which a bond breaks. As shown in Figure 1, Burger's model consists of a Maxwell model element and Kelvin element. Aggregates are modeled as pure elastic and a spring element is employed to represent the mechanical behavior. Up to three types of contacts will be addressed in this research study: 1) within asphalt materials, 2) within and between aggregates, and 3) between asphalt and aggregates.
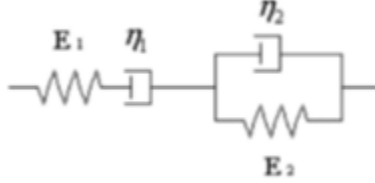
Figure 1. Burger's Model (After Liu et al., 2009)

Figure 2 illustrates the stiffness model between an aggregate element (A) and an asphalt element (B) in normal direction, the model stiffness parameters can be expressed as:

$$K_{mn} = \frac{k_{mn}^B k_n^A}{k_{mn}^B + k_n^A}$$

$$C_{mn} = c_{mn}^B \qquad K_{kn} = k_{kn}^B \qquad C_{kn} = c_{kn}^B$$

where the parameters in the equations are the stiffness parameters and viscosities of the spring and dashpots elements as shown in Figure 1. Similar relations can be derived for the aggregate-aggregate contact and asphalt-asphalt contact, as well as for stiffness in shear (Liu et al. 2009). Furthermore, the micro-scale properties can be calculated for aggregate-asphalt contact in normal direction using the following equations,:

$$K_{mn} = \frac{2EE_1}{E+E_1}\begin{cases} t \ (2D) \\ L \ (3D) \end{cases} \qquad C_{mn} = 2\eta_1 \begin{cases} t \ (2D) \\ L \ (3D) \end{cases}$$

$$K_{kn} = 2E_2 \begin{cases} t \ (2D) \\ L \ (3D) \end{cases} \qquad C_{kn} = 2\eta_2 \begin{cases} t \ (2D) \\ L \ (3D) \end{cases}$$

where E_1, E_2, η_1, and η_2 are Burger's model parameters shown in Figure 1, while E is Young's modulus for the aggregate, t is the discrete element thickness in 2D, and L is

the beam length in 3D. Again, similar relationships can be derived for other types of contacts and for the shear direction.
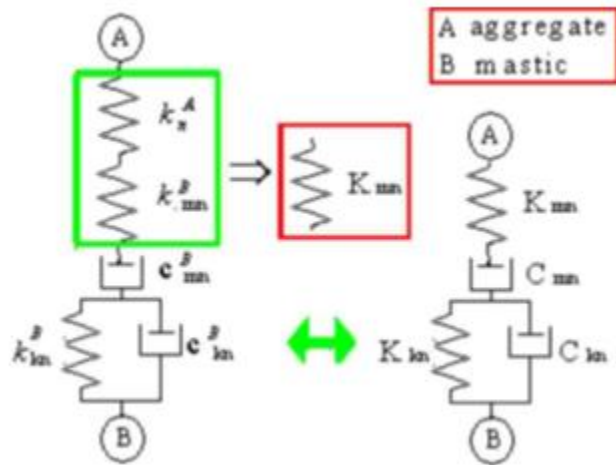
Figure 2. Burger's model parameters between asphalt and aggregate elements. (After Liu et al., 2009)

Overlay Tester (OT)

The overlay tester was originally designed by Germann and Lytton (1979) to study the opening and closing of joints or cracks. Figure 3 illustrates the main components of the OT, which consist of a fixed steel plate and a movable steel plate, the loading simulates the opening and closing of joints/cracks. Zhou and Scullion (2005) improved the design of the OT and introduced as a routine laboratory test for pavement design and evaluation. One of the main improvements was the use of 150 mm (6 in.) samples, rather than the long beams required by the original OT test (Zhou and Scullion, 2005). Bennert (2009), Bennert et al. (2009), Bennert and Dongré (2010), Hajj et al. (2010), and Bennert et al. (2011) found the modified testing procedure to be reliable and practical test for evaluating asphalt mixtures resistance to cracking. Walubita et al. (2012 and 2013) indicated that the variability of the test can be minimized if certain key variables are controlled, such as: drying method, glue quantity, number of sample replicates, air voids, sample age at the time of testing, and temperature variations. Some of the recommendations include:

4

- Testing five replicates and reporting the best three results instead of the current practice of testing three samples to improve repeatability.

- Oven drying of the OT specimens at a maximum temperature of 40 ± 3°C (104 ± 5°F) for a minimum of 12 hours to constant weight is preferable to air drying.

- OT specimens having air-void values between 6.5 percent and 7.5 percent gave the most repeatable results.

- The specimens need to be tested within 5 days of molding, i.e., specimen sitting time between moldings and testing should not exceed 5 days.

- The use of 16.0 ± 0.5 g or 16.0 ± 0.5 ml of Devcon 2-part, 2-ton epoxy for gluing the specimens to the old OT testing plates is the most economical and gives the most repeatable results.

- No conclusive trend was displayed by the OT variability with changing test temperatures. However, the tolerance limit should not exceed ±2 F.

- The OT result variability showed a slight improvement with decreasing opening displacement. However, changing these loading parameters also requires validation with field performance data. Therefore, the current practice of 0.025 in. opening displacement is recommended.
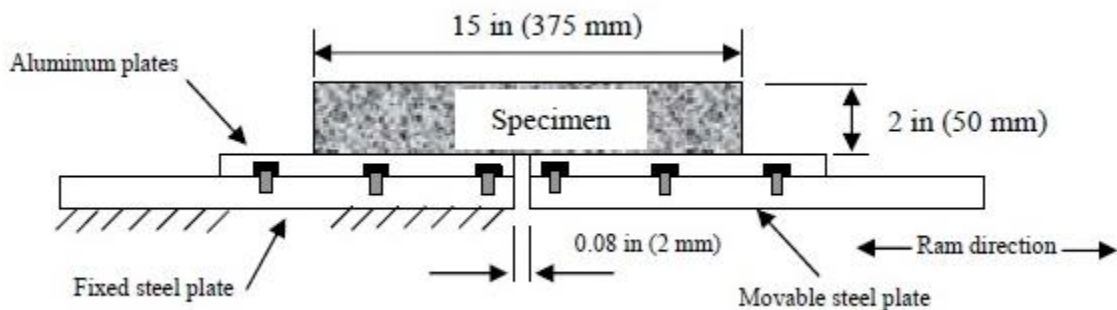
Figure 3. Overlay Tester (After Zhou and Scullion, 2005)

Koohi et al. (2013) presented an analysis method based on the viscoelastic fracture mechanics and 2D finite-element (FE) modeling to predict the actual crack growth rate in asphalt mixes, both the in laboratory compacted and field samples by using the OT. The FE simulation results showed that the energy release rate decreased as the crack

grew. They indicated that the OT could be used as a rapid and robust test for determining the fracture and healing properties of asphalt mixes. The accuracy and repeatability of this method demonstrated to be superior to previous methods using the same test apparatus. In addition, the analysis of the crack growth and pseudo-work dissipation produced both fracture and healing properties.

Objectives

The main objective of this study is to develop a numerical model supported with imaging techniques to study asphalt mix crack resistance with DEM. Both homogenous and heterogeneous models were developed. The following tasks were performed to achieve this objective:

- Materials Selection: materials and mixes were selected to cover wide range of aggregate gradations, strength, and shape properties.
- Development of Numerical OT: discrete element model of OT was developed for homogenous and heterogonous samples. Additionally, three options for applying boundary conditions were considered.
- Materials Calibration: materials and mixes selected were calibrated in DEM to provide material properties required for the OT numerical model. Laboratory testing results for rock masses in compression and split tensile, and asphalt mixes split tensile were used for the calibration.
- OT Analysis: OT-DEM model simulations, for homogenous and heterogonous, results were analyzed to assess the damage within the samples during the first two cycles of loading and compare it to the damage at ultimate failure for monotonic loading case.

Materials and Mixes

Three mixes and three types of aggregates as illustrated in Table 1 were selected for this study. These gradations (see Figure 4) provided significantly different aggregate structures. The designations of these mixtures follow TxDOT classification of mixtures. The PFC is sometimes referred to as open-graded friction course (OGFC). It is an open-graded mixture with a high percentage by weight of coarse aggregates. It is composed

of 89% aggregates larger than a No. 8 sieve. The Superpave-C mixture is a well-graded mixture that consists of roughly 35% coarse aggregates and 65% fine aggregates. The coarse matrix high binder (CMHB-C) mixture is a gap-graded mixture that is very similar to SMA in its volumetric properties. It is composed of about 63% coarse aggregates and 37% fine aggregates. The research team has access to X-Ray CT images for the mixes outlined in Table 1, in addition to all material properties required for the modeling, relevant testing results available are illustrated in Table 2.

Table 1. Numerical modeling matrix

Aggregate Type	Superpave-C	CMHB-C	PFC
Hard Limestone	X	X	X
Soft Limestone	X	X	X
Granite	X	X	X
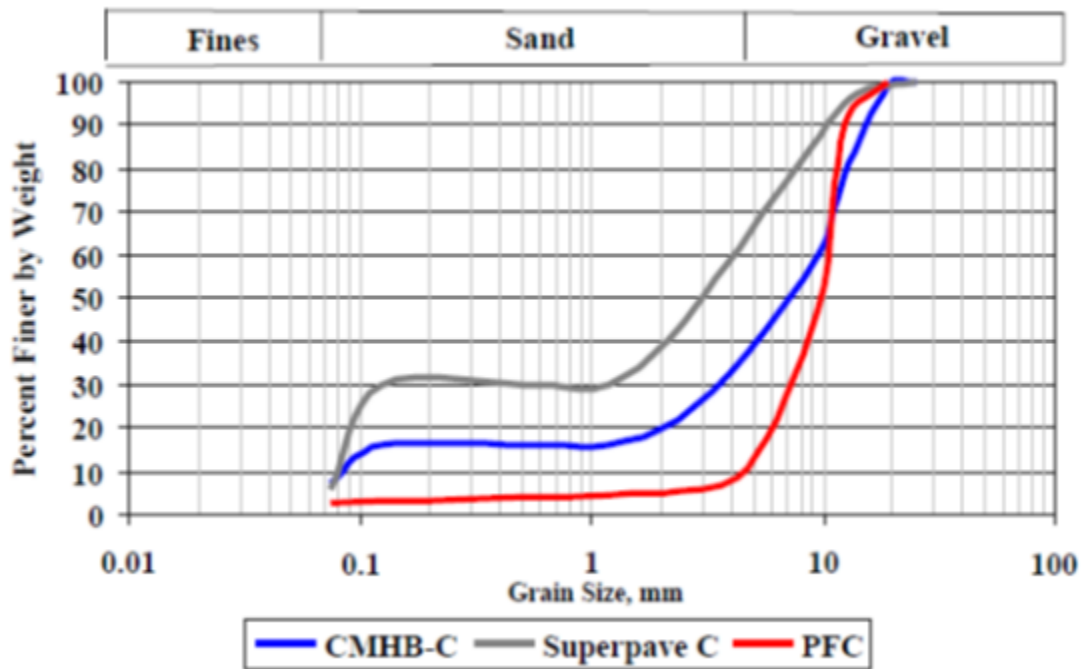
Figure 4. Aggregate Gradation (After Alvarado et al., 2007)

7

Table 2. Available Laboratory Testing Results

| Material	Testing Results Available
Rock Masses	Splitting Tensile, Compressive Strength, and Modulus
Asphalt Mixes	X-Ray Imaging and Splitting Tensile

OT Model Development

The objective this task is to develop a DEM utilizing random packing schemes to model the specimen within an overlay. This was achieved in four steps. Step 1 focused on developing material-genesis for asphaltic materials. While material-genesis for rock mechanics applications has been the focus of ongoing research studies for many years, and is fairly developed, most of asphaltic materials advances in this field are limited to simplistic packing schemes, or by simply adapting the rock mechanics approach. The need for material specific material-genesis procedure is very important and the needs for it stems from the fact that the internal structure of asphaltic materials are different from those of solid rocks. The focus in this task was on producing material-genesis for homogenous and heterogonous asphaltic materials. The one-phase asphalt material-genesis was not expected to be challenging as it was a slight modification of the rock mechanics model. Solid rock material-genesis was based on representing the rock material with dense-packing of nonuniform circular (2D) or spherical (3D) discrete elements that were bonded at the contact points. The following is a summary of the material-genesis procedure (Potyondy and Cundall, 2004):

1. Create initial assembly: a material vessel created and filled with dense packing of discrete elements with a specific size range and no friction. The elements are placed at half their target size, such that no two elements overlap, the particle size is then doubled, and the system is allowed to rearrange under zero friction conditions (Figure 5)
2. Reduce locked-in forces: the size of all the elements is reduced uniformly to achieve minimum locked-in forces without compromising the elements connectivity.

8

3. Reduce/Remove floating particles: a particle with less than three contacts is considered floating and is undesirable for a dense-packed assembly. Floaters removal can be achieved by expanding and moving floaters until every element has the minimum number of contacts.

4. Install bonds: bonds are then installed throughout the elements assembly. This specific procedure uses a normal distribution based on average and standard deviation value of the bond strength.

a)

b)

c)

d)
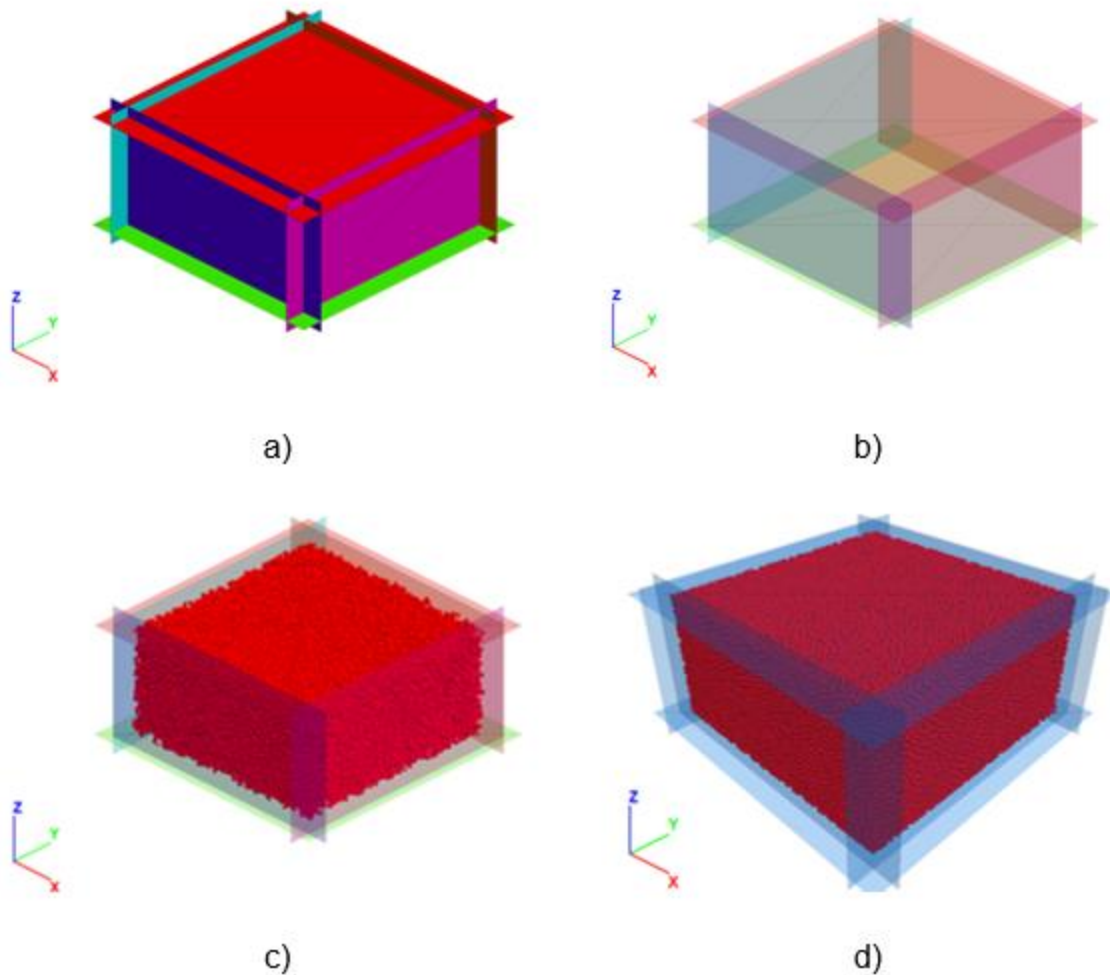
5. Remove from material vessel: the next step is to remove the assembly from the materials vessel and allow it to relax (Figure 6-a).

6. Extract OT sample: the final step is trim the material to the OT sample shape by deleting excess elements (Figure 6-b, c, d, and e)
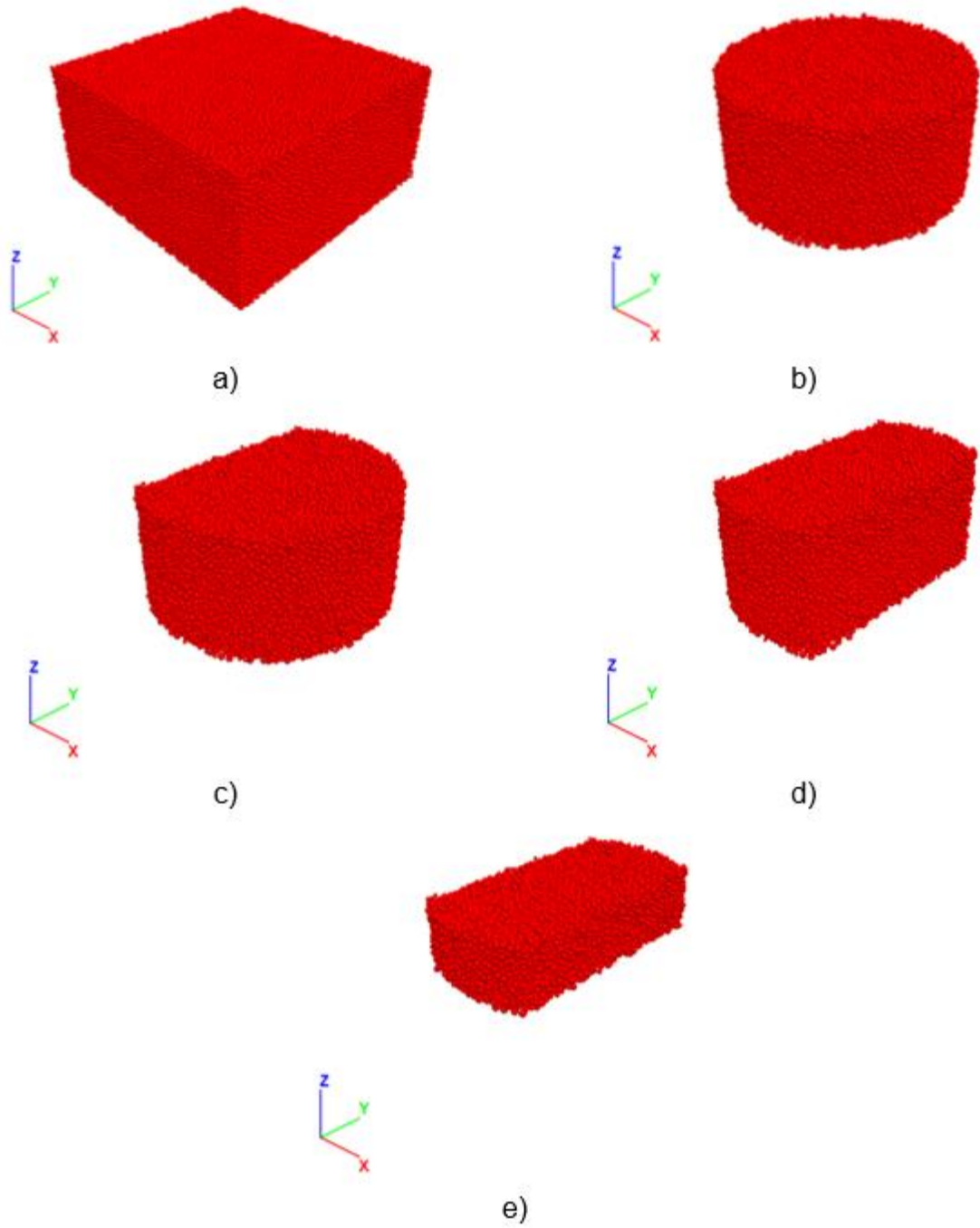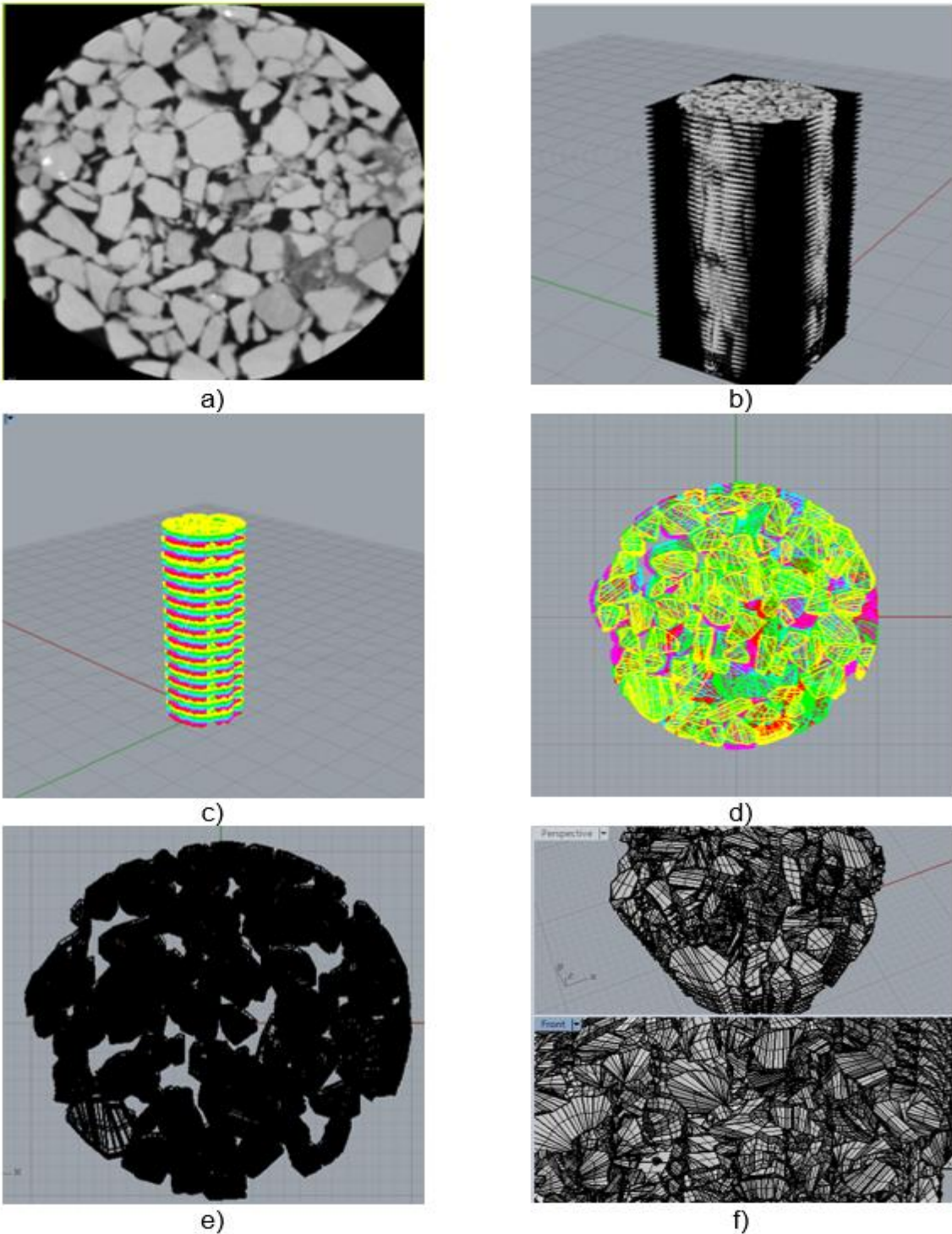
Figure 5. Overlay Tester Development: a) Material Vessel, b) Transparent Material Vessel, c) Initial Elements Generated, d) Elements Rearranged under Zero Friction

Figure 6. Overlay Tester Development: a) Material Removed from Vessel, b) Cylinder Extracted, c) Left Side Trimmed, d) Right Side Trimmed, e) OT Sample

Step 2 focused on expanding the model from homogenous to heterogonous. This was achieved by using X-ray images available from previous research project (Alvarado et al., 2007). The X-ray images are stacked to form the three-dimensional representation of the asphalt mixes internal structure. An example of an image taken by the X-ray CT is illustrated in Figure 7a. The images were then imported to a commercially available CAD software (Rhino 3D). As each image is imported into the software and placed in the appropriate position, a clear "Top View" of the Cylinder is shown at such height (Figure 7b). For each layer, every aggregate particle was outlined to generate 2D meshes as illustrated in Figures 7c and 7d. Finally, the 2D meshes for each of the aggregates were combined to create the 3D aggregate representation (Figures 7e and 7f). The 3D aggregate representation was then transferred from Rhino 3D to PFC3D software as a geometry. Figures 8a through 8d illustrate snapshots of a 3D geometry from the z-axis view, y-axis view, x-axis view, and the perspective view, respectively. Once the geometry was transferred and located within the OT-DEM sample (Figure 8e), the particles within the model occupying the same location of the geometry were labeled as aggregates, and thus the material properties could be specified for aggregates and mastic separately, as illustrated in Figure 8f.

The third step in the development of the OT-DEM was the addition of the loading plates, three methods were considered. The first method was to add the loading plates as rigid walls in DEM, the walls were then glued to the OT sample by introducing a very high contact bond. The second method was to represent the plates using DEM particles, and this required repeating Step 1 to produce the required shape. Finally, the third method was based on applying the boundary conditions to the bottom of the OT sample. These conditions were: fix the particles in all directions for the fixed plate side, and apply the velocity vector to the moving plate side. Figure 9, illustrates the three cases. All three methods produced similar results; however, the computational time was significantly different, with the third method requiring the least time to run the simulation. The loading-unloading curve is shown in Figure 10, the maximum displacement and

displacement rate are selected to match the current test standard, however, the model is flexible to accommodate any changes.

Figure 7. Development of 3D Aggregate Structure
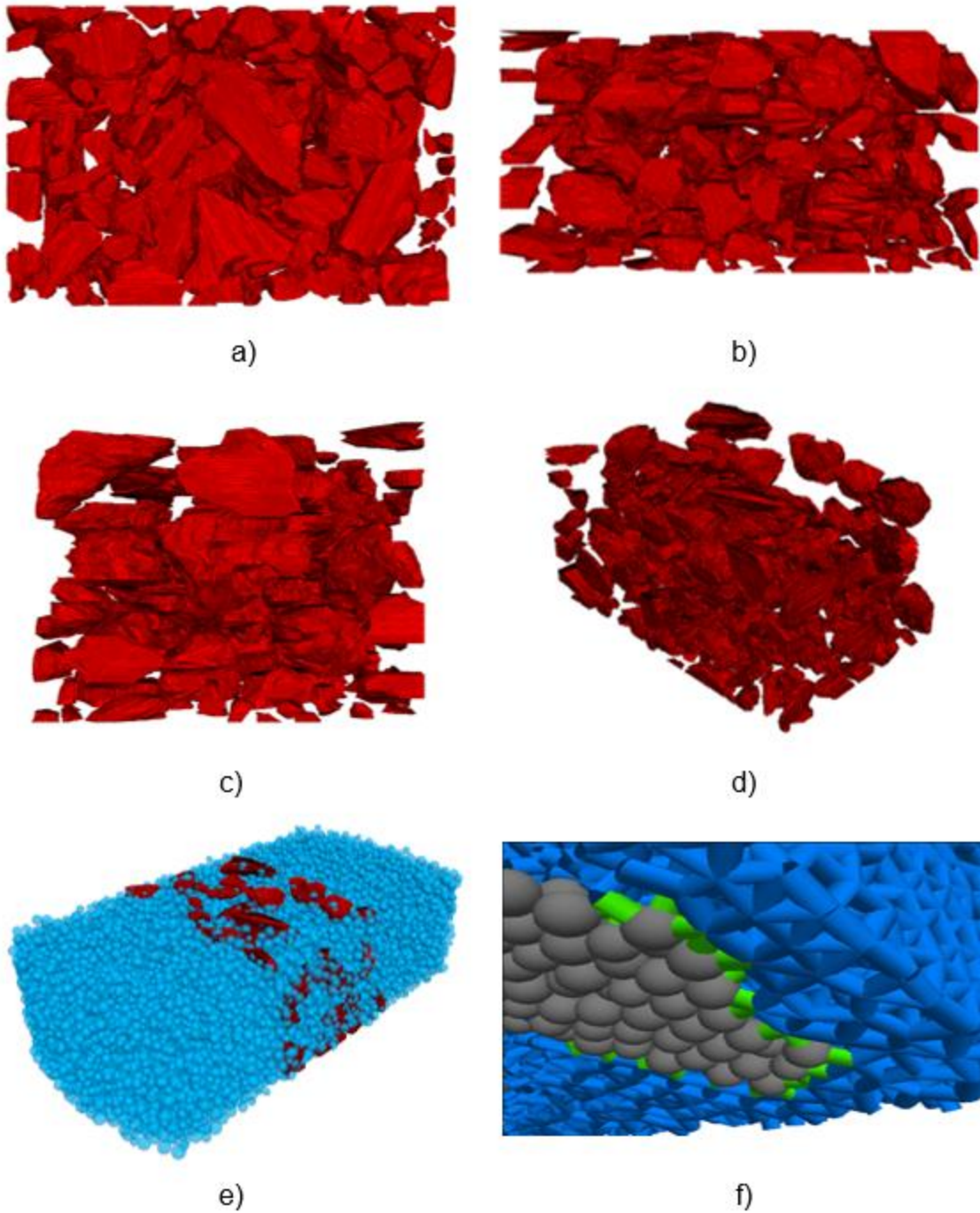
Figure 8. Heterogeneous Overlay Tester Development: a) 3D Aggregate Structure z-axis View, b) 3D Aggregate Structure y-axis View, c) 3D Aggregate Structure x-axis View, d) 3D Aggregate Structure Perspective View, e) 3D Aggregate Structure Transformed into OT Sample, f) Aggregate-Mastic Interface.
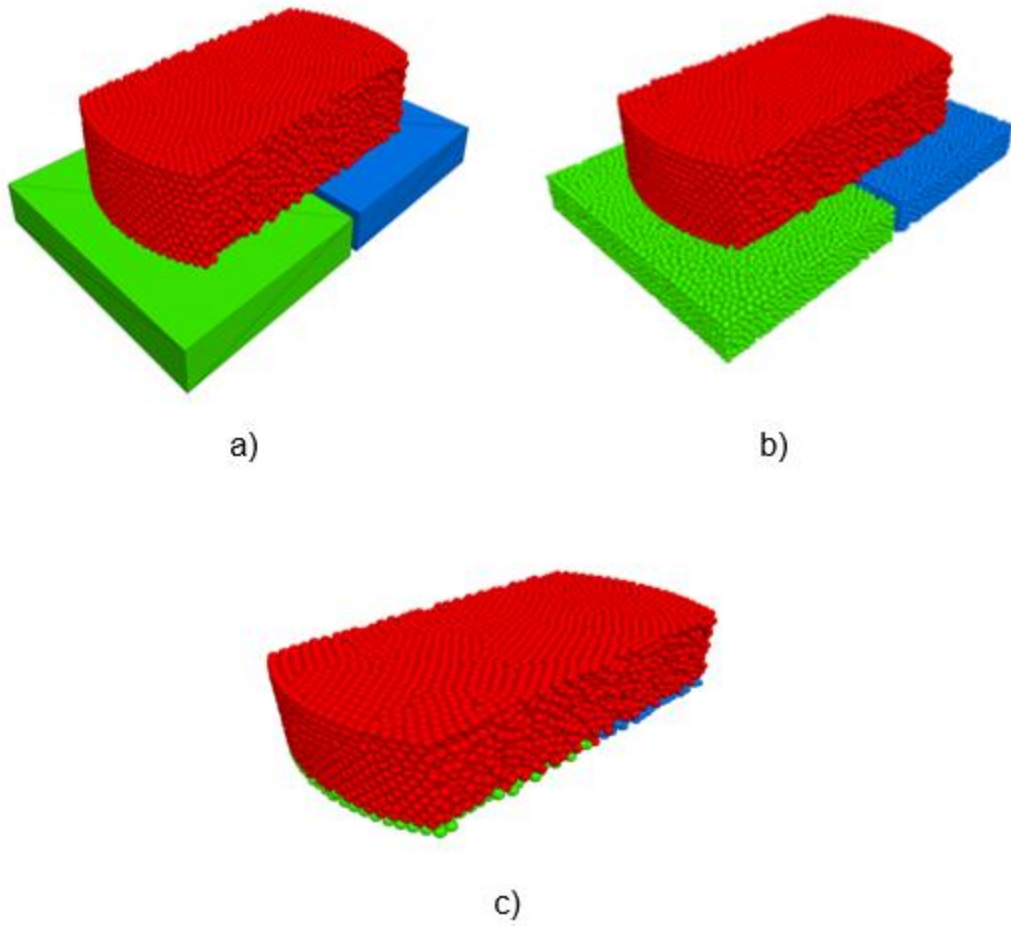
Figure 9. Overlay Tester Development: a) Rigid Wall Loading Plates, b) Discrete Element Particles Loading Plates, c) Boundary Condition Loading Plates
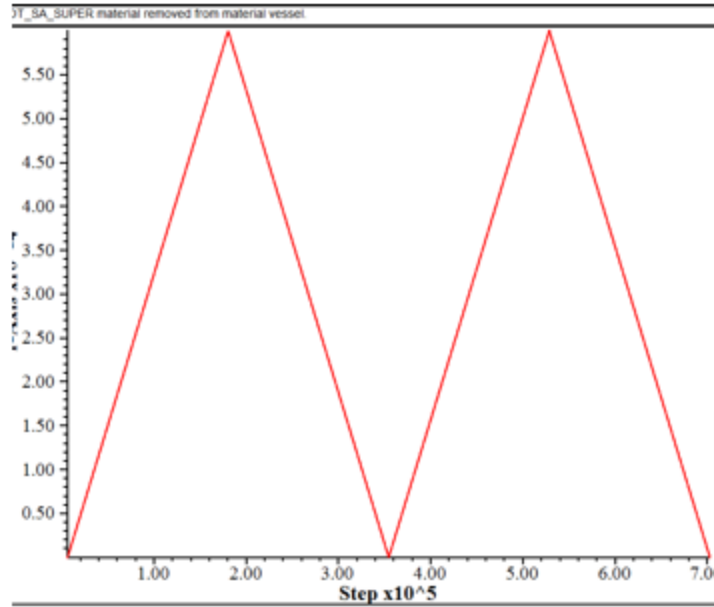
Figure 10. Overlay Tester Two Cyclic Loads

The final step was to study the effect of the resolution on the OT simulation results. The resolution in this context is the diameter of the discrete element particles. Although, the overall strength could be achieved by any resolution, finer resolution would provide better representation of the internal forces as well as the crack initiation and propagation processes, while coarser resolution will provide faster simulations. Figure 11 illustrates the OT-DEM samples for different resolutions; the number underneath each sample is the range of the discrete particles radius specified in the first step of the material-genesis procedure. To compare the results from different resolutions, all samples were loaded and the internal stresses were tracked at pre-specified locations, the analysis indicated that radius range of 1 to 2 mm is sufficient to capture the internal stresses, while coarser resolutions do not produce reliable results.

0.4 to 0.6   0.6 to 0.8   0.8 to 1

1 to 1.2   1.2 to 1.4   1.4 to 1.6

1.6 to 1.8   1 to 2   2 to 3

3 to 4   4 to 5   5 to 6

6 to 7   7 to 8   8 to 9
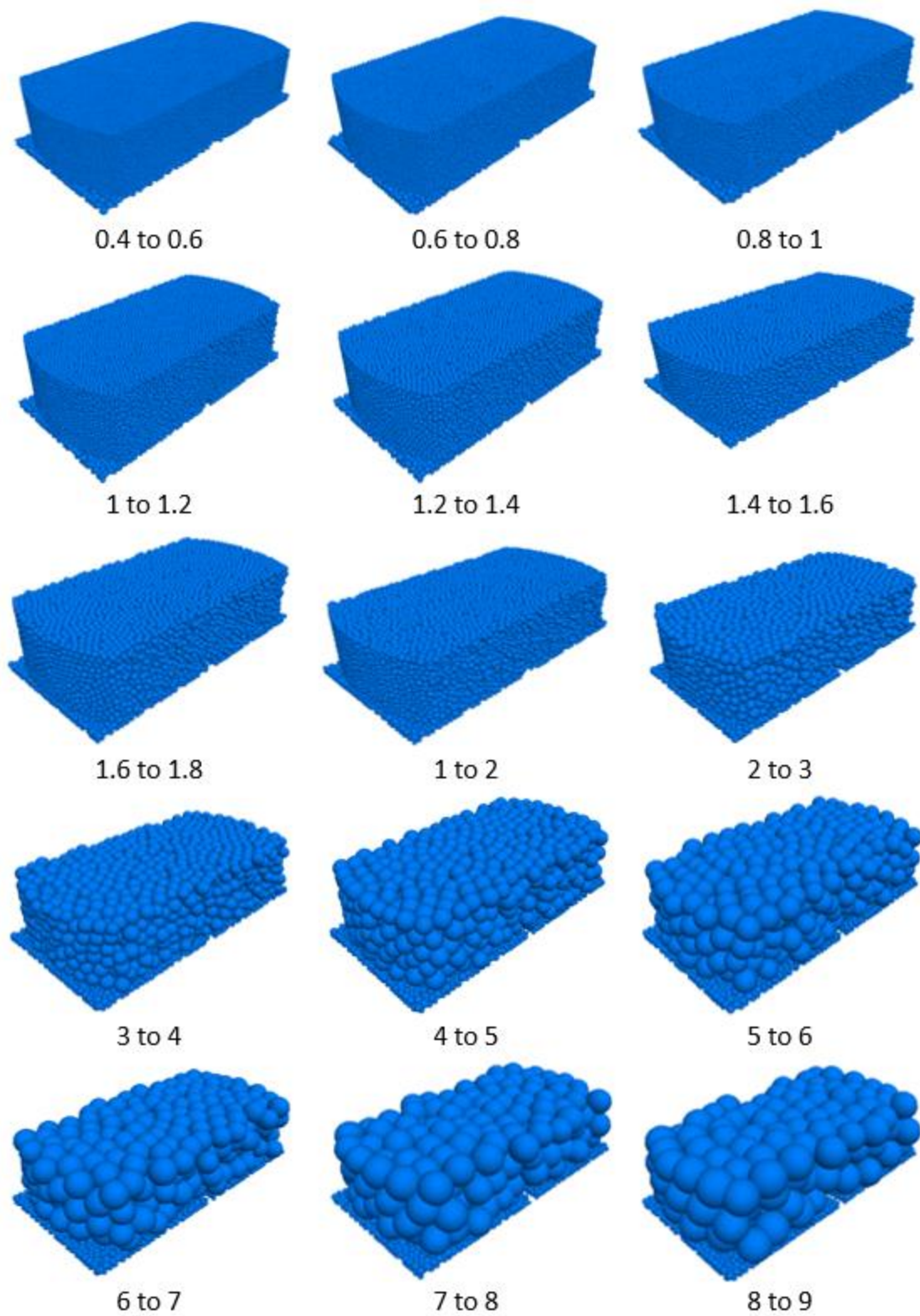
Figure 11. Overlay Tester Development: Fine to Coarse Resolutions

Aggregate and Asphalt IDT Calibration

The focus of this task was to calibrate the material properties. For strictly continuum models such as FEM, the material input properties can be derived directly from laboratory testing. In DEM, which synthesizes macro continuum material behavior from the interactions of micro discrete elements, the input properties usually are not known. The relation between model parameters at the micro scale and material properties measured in the laboratory is only known for simple packing arrangements (Potyondy, 2007). For the general case of random packing and arbitrarily sized discrete elements, the relation is found by calibration. The calibration process entails setting the micro parameters of the model, such that the simulated test results match material properties measured in similar tests. It is important to clarify that the DEM approach is not sensitive to the elements size, i.e. coarse- or fine- resolution of discretization. The effect of discretization resolution is eliminated by employing scaling relations when specifying model micro parameters. The calibration process was performed for homogenous and heterogeneous asphalt mixes. Calibrating heterogeneous asphalt mixes required calibrating rock tests first, the following subtask were performed to complete this task:

1. Calibration of homogenous asphalt mixes – Split tensile test
2. Calibration of rock masses – compressive strength, splitting tensile, and modulus
3. Calibration of heterogeneous asphalt mixes – splitting tensile

Homogenous asphalt mixes

As mentioned in the previous section, splitting tensile laboratory results for the nine asphalt mixes included in this study were available to the research team from a previous study (Alvarado et al., 2007). The objective of this task was to calibrate the material properties of the DEM model to match the laboratory test results. The DEM model followed the same loading rate and boundary conditions of the laboratory test. As discussed in the background, DEM requires material properties in shear, and normal directions, in addition to the bond strength. The calibration focused on matching the maximum load and the displacement at that load. Figure 12, shows an example of the load-displacement curve for the Superpave-Hard limestone mix, while Figure 13 illustrates the DEM model. The normal and shear bond strengths were varied until the

numerical results matched the experimental strength measurements (maximum load). While the contact stiffness among the model elements was varied until the model displacement at the maximum load matched the experimental measurements. This required conducting iterative analysis to determine the parameters that had the best match with both the maximum load and the displacement at the maximum load. The results in Figures 14 and 15 show the comparison between the DEM results and the experimental results for the maximum load and displacement at maximum load, respectively. The indirect tensile model for the asphalt mixes compared very well with the experimental results.
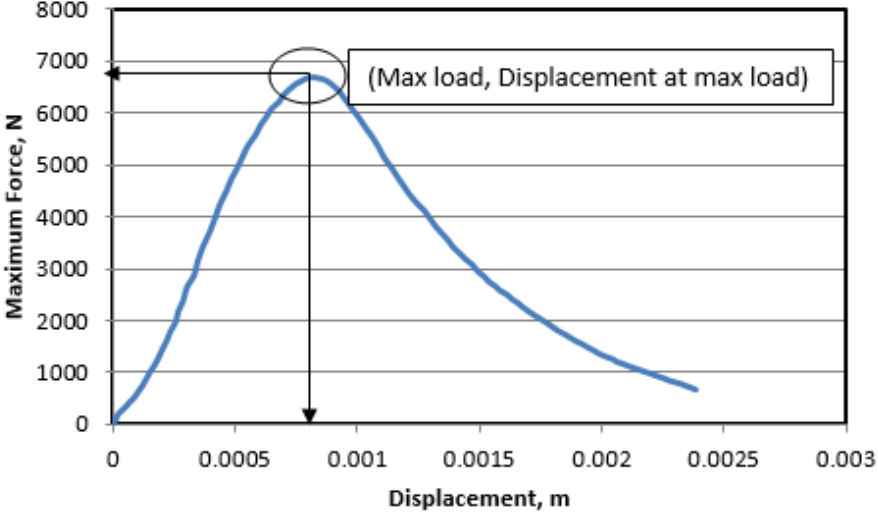
Figure 12. Indirect Tensile Load-Displacement Curve
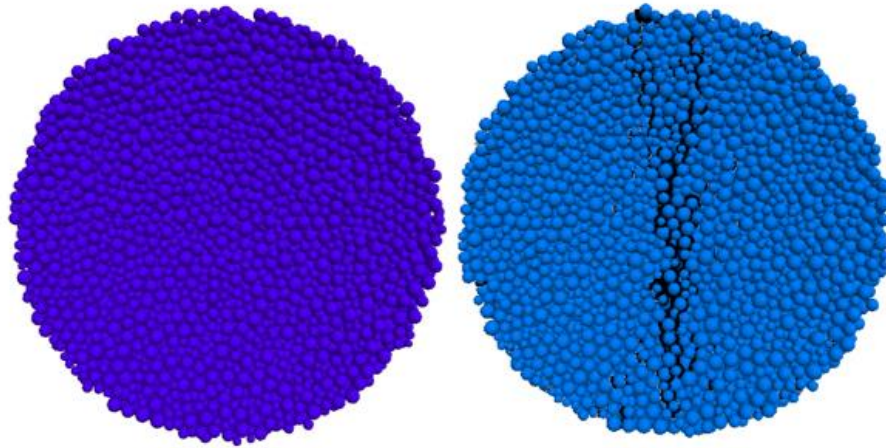
Figure 13. Indirect Tensile DEM Model (Black Line Represent Fracture Post Loading)

▲ SuperPave_Granite	✕ SuperPave_Soft Limestone	✕ SuperPave_Hard Limestone
● CMHB_Granite	+ CMHB_Soft Limestone	– CMHB_Hard Limestone
– PFC_Granite	◆ PFC_Soft Limestone	◆ PFC_Hard Limestone
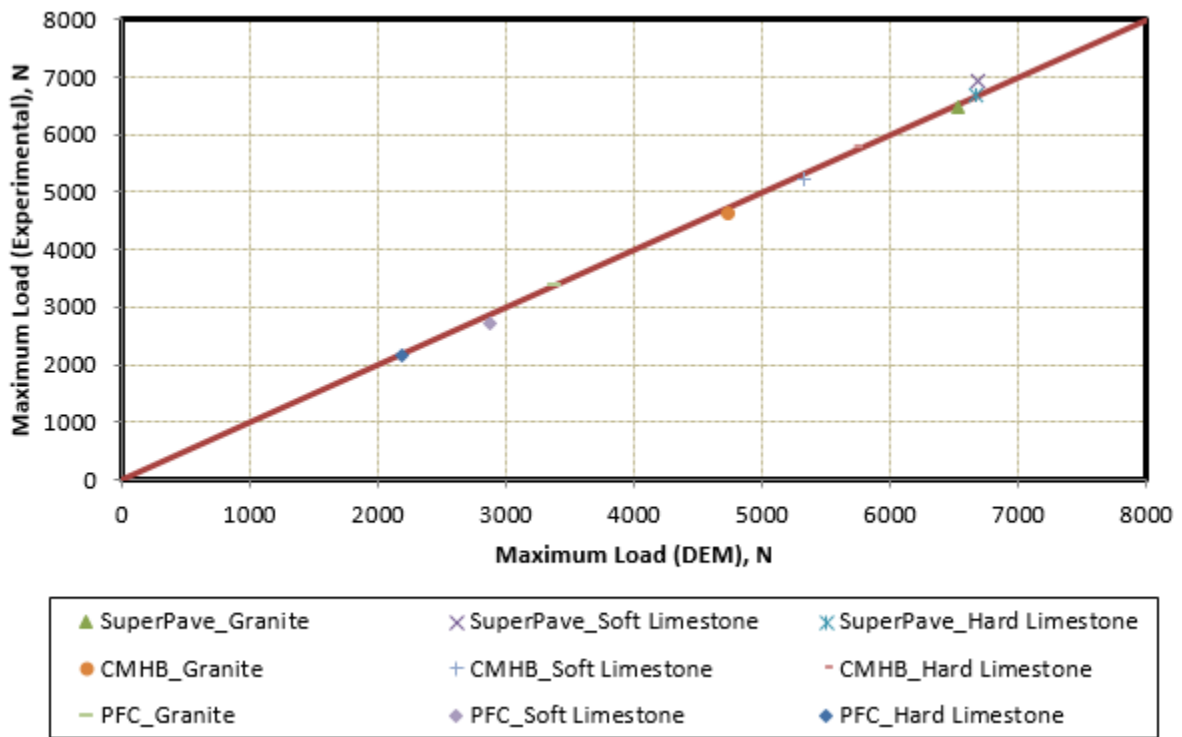
Figure 15. Indirect Tensile Displacement at Maximum Load Comparison

Rock masses testing calibration

DEM was used to model the modulus test, compressive strength test and indirect tensile strength of rock samples for the three aggregates used in this study. Figure 16 illustrates the DEM model for compression and splitting tensile tests. The aggregate contact stiffness and strength in the model were determined such that the model results matched the experimental measurements.
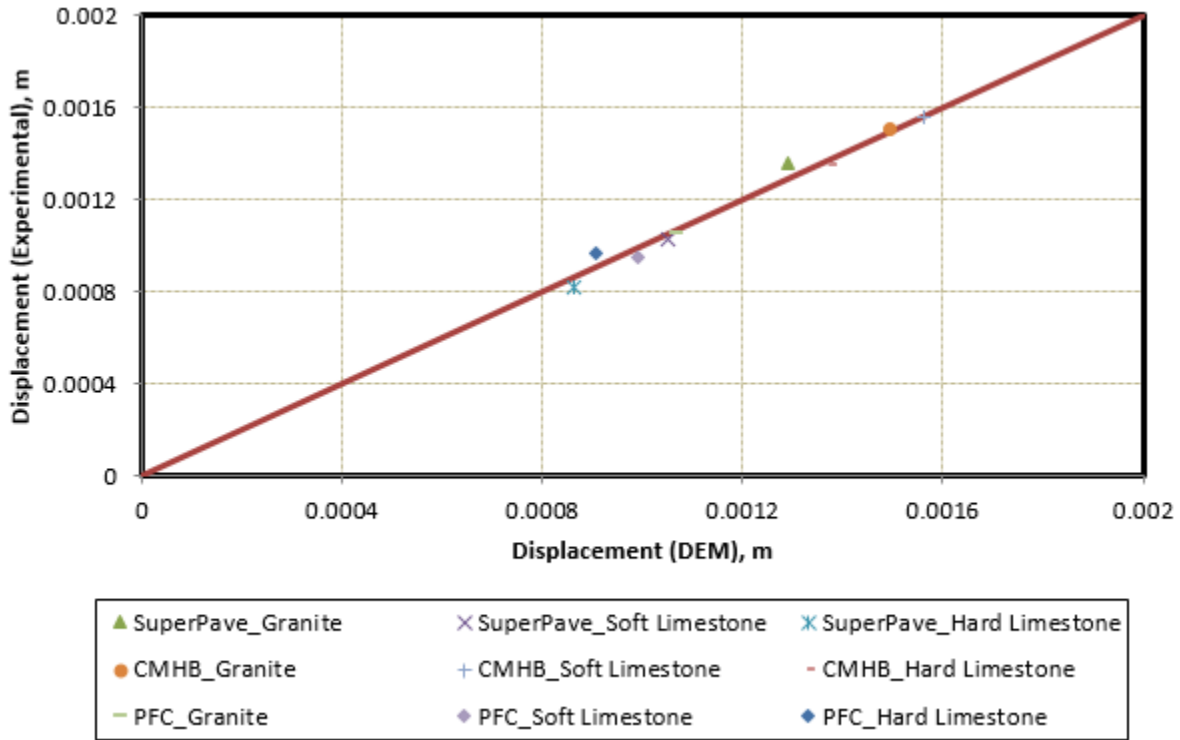
The contact stiffness among the model balls was varied until the model stiffness matched the experimental stiffness measurements. The normal and shear bond strengths were varied until the numerical results matched the experimental strength measurements. Similar to the asphalt mixes, this required conducting iterative analysis to determine the parameters that had the best match with both compressive and split tensile tests. The results of the compressive strength were more dependent on the shear strength, while the indirect tensile strength was more dependent on the tensile

normal strength. A comparison between the experimental and modeling results are shown in Figures 17 through 19.
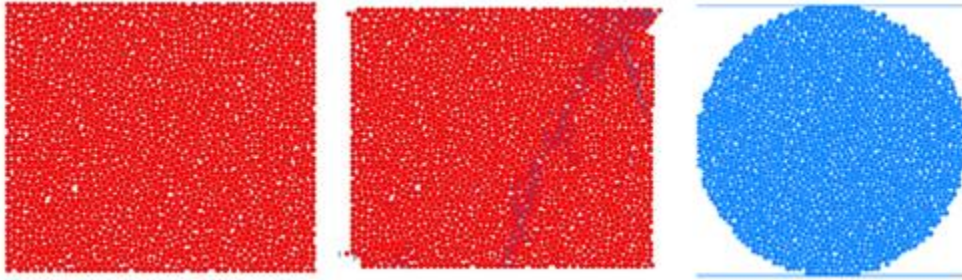
Figure 16. **Rock Masses DEM Compression and Indirect Tensile Models**
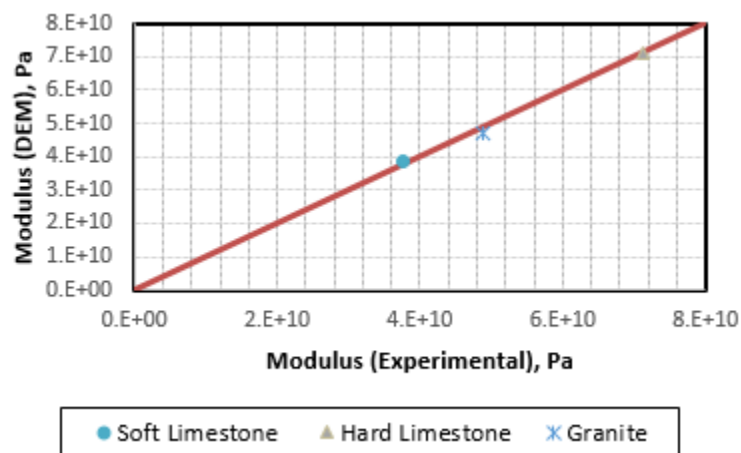
Figure 17. **Rock Masses Modulus Comparison**
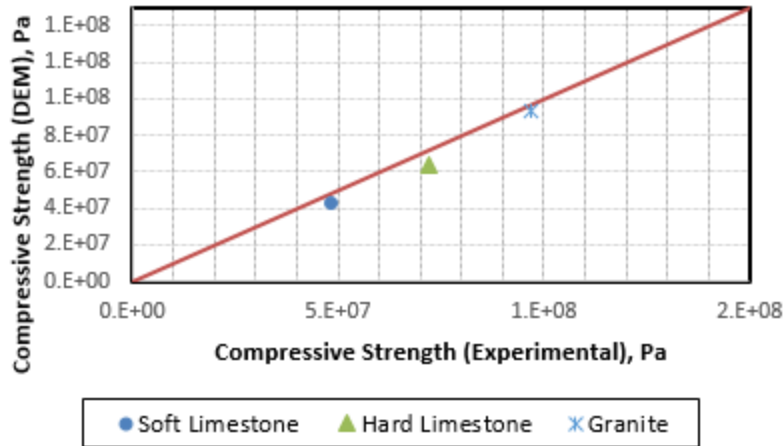
Figure 18. **Rock Masses Indirect Compressive Strength**
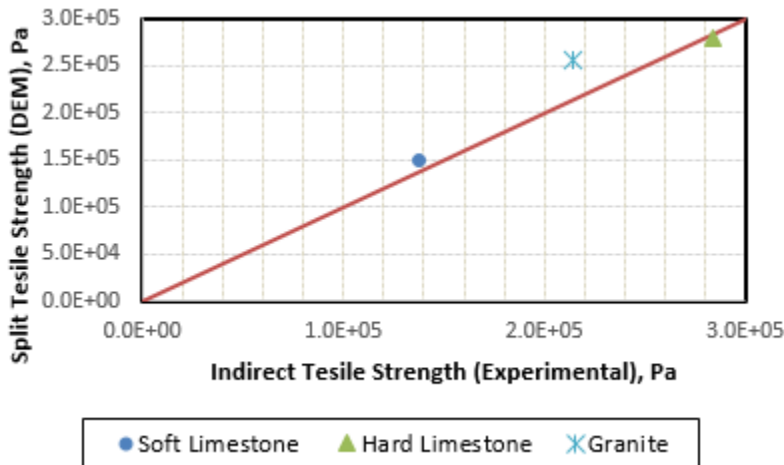
Figure 19. **Rock Masses Indirect Tensile Strength Comparison**

Heterogeneous asphalt mixes

Heterogeneous DEM models for asphalt mix split tensile test are shown in Figure 20-a through c for Superpave-C, CMHB-C, and PFC, respectively. Aggregate parameters obtained from the previous step (Rock masses testing calibration) were used to represent the aggregate within the asphalt model. The mastic properties were determined such that the model results match the indirect tensile strength of the mixes. Figure 21 illustrates the comparison between the DEM results and the experimental results. The indirect tensile model for the bituminous mixes compared very well with the experimental data.
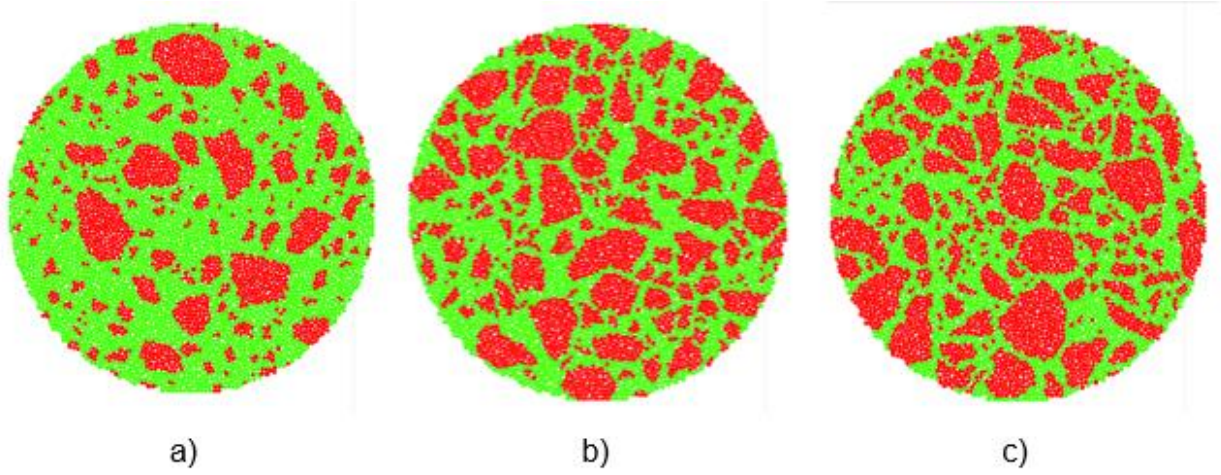
Figure 20. DEM Models: a) Superpave-C, b) CMHB-C, c) PFC
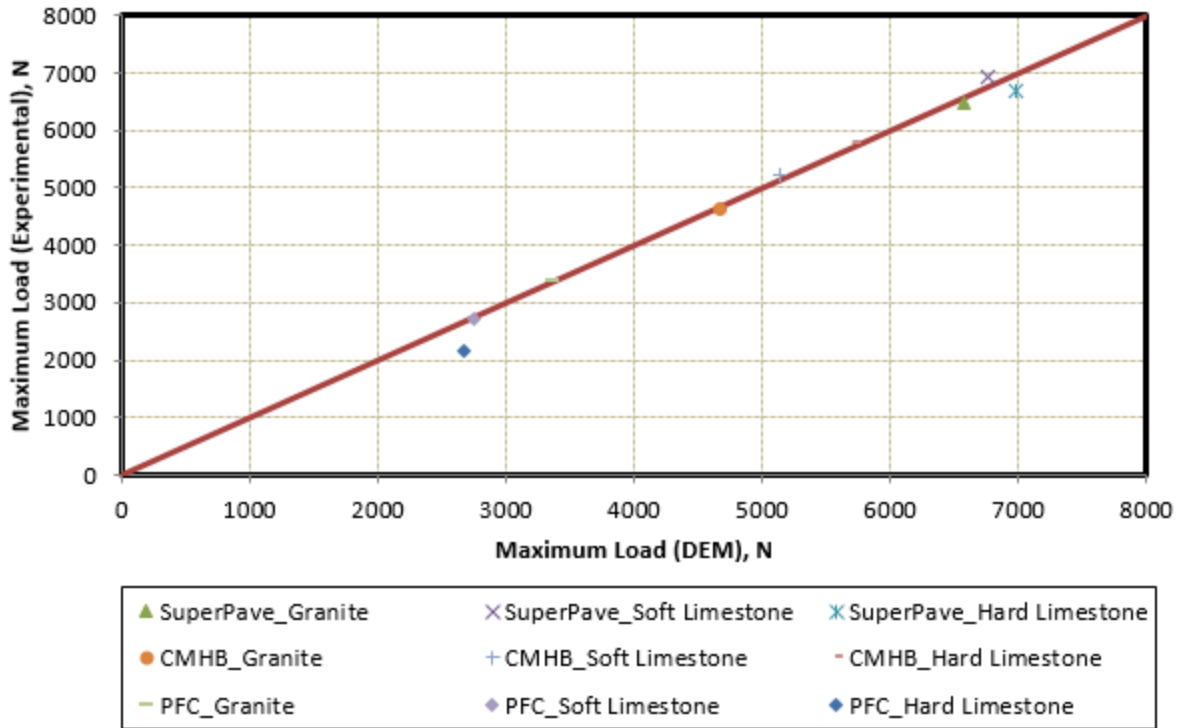
Figure 21. Indirect Tensile Maximum Load Comparison-Heterogeneous DEM

OT Analysis

The final task in this project was to numerically study the OT test, the main focus was on the damage induced within the first loading cycle, which some laboratory testing results has shown is significant. Both homogenous and heterogeneous asphalt cases were considered. The DEM material parameters from the calibration task were used. Figure 22, illustrates the loading cases considered for the homogenous samples; half-cycle, one-cycle, one and half-cycle, 2 cycles, and monotonic loading until failure. Figure 23 depicts an example of OT sample after failure from two views. Initially the analysis focused on the damage within the sample represented by the number of active contact bonds in the center of the sample. A visual representation of the bonds within the OT sample is shown in Figure 24 a and b. A cutting plane was specified with the origin at the center of the sample (0, 0, 0) and normal vector in the y direction (0, 1, 0), once this is applied only the bonds in the center of the sample are visualized (Figure 24 – c and d). This techniques is only for visualizing and counting purposes, in other words

the bonds within the sample in other locations still exist. Figure 24-e shows an example of the active bonds in the center of an OT sample after one loading cycle.
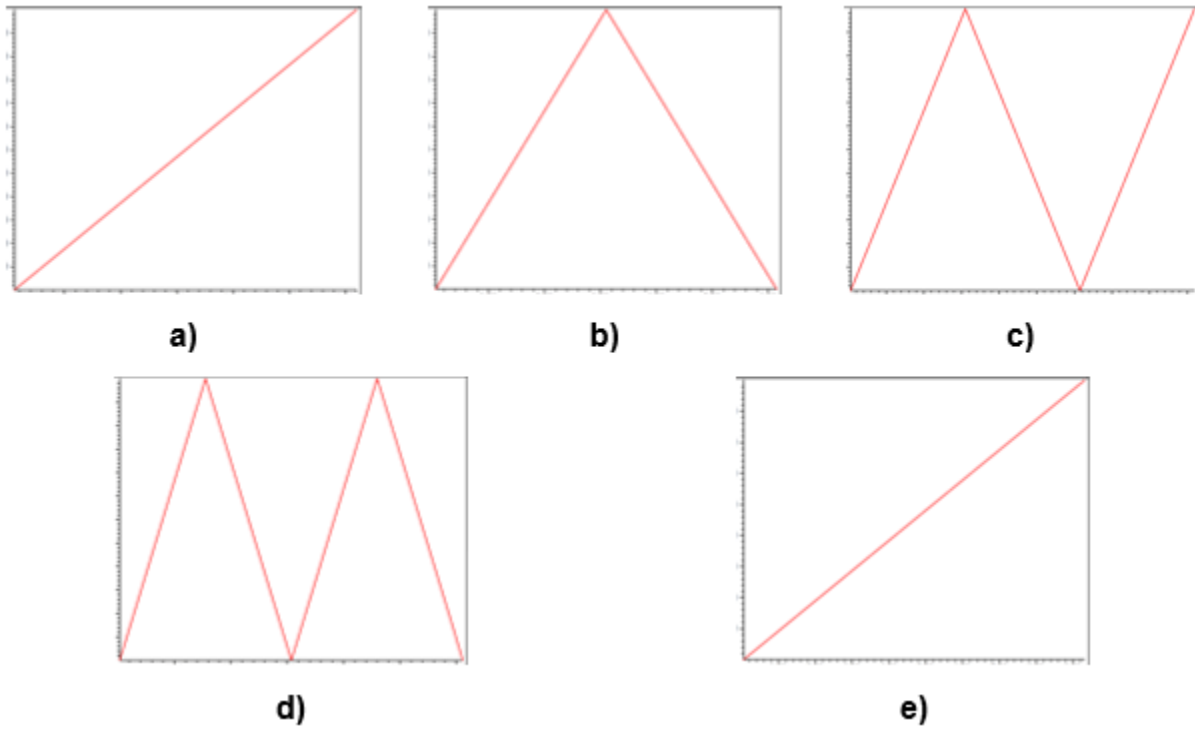
Figure 22. Overlay Tester DEM Loading Schemes: a) Half-Cycle, b) One Cycle, c) One and a Half-Cycle, d) Two Cycles, e) Monotonic Loading
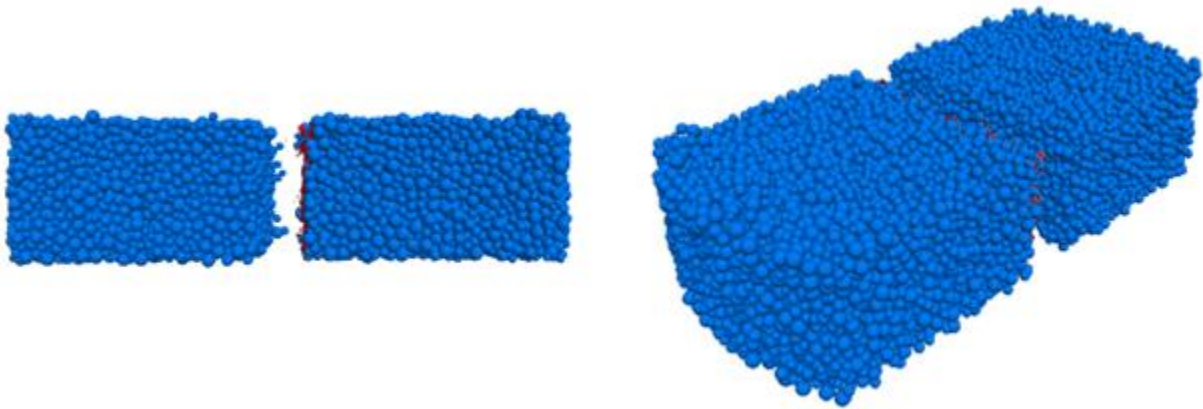
Figure 23. Overlay Tester Failed Sample
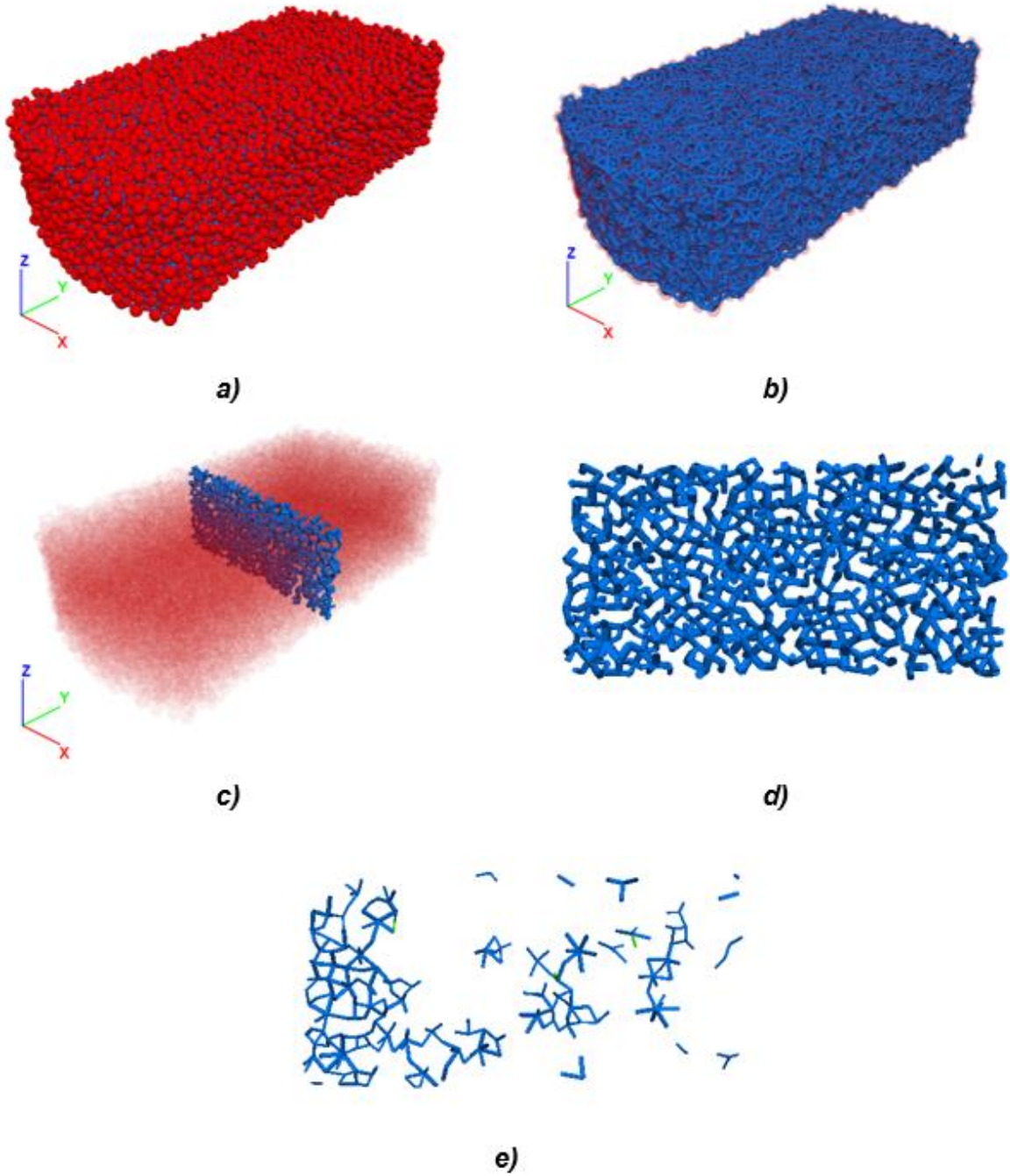
Figure 24. Overlay Tester Development: a) OT Sample, b) OT Sample Bonds, c) OT Sample Center Bonds, d) Center Bonds Isolated, e) Center Bonds after One Loading Cycle

Table 3 lists the number of active for the nine aggregate-mix combinations considered in this study. The unloaded number represent the number of the active bonds at cutting plane before the simulation start, the table also illustrates the active bonds after one loading cycle, two loading cycles, and monotonic loading until complete failure. While the results of the one and two cycle looked promising, the monotonic results were not yielding zero active contacts, which is inconsistent with the fact that the sample was loaded up until complete failure (Figure 23). After close inspection of the model, the researchers noticed that the cutting plane was still including some of the active bonds from the fixed side of the OT-sample, i.e. the plane is not moving to stay in the center of the sample. When the plane was moved to be in center of the sample, which is no longer (0, 0, 0) after loading, the correct zero active bonds for the monotonic loading case were obtained.

Table 3. DEM OT Sample Active Bonds

| Aggregate – Mix Type	# of Active Bonds			
	Unloaded	One Cycle	Two Cycles	Monotonic*
Hard Limestone – PFC	890	544	544	0
Hard Limestone – CMHB	870	239	239	0
Hard Limestone – Superpave	893	658	658	0
Granite – PFC	879	494	494	0
Granite – CMHB	879	459	459	0
Granite – Superpave	867	277	277	0
Soft Limestone – PFC	873	452	452	0
Soft Limestone – CMHB	878	457	457	0
Soft Limestone – Superpave	886	566	566	0

Monotonic numbers adjusted by moving the cutting plane

Due to the possibility of obtaining inaccurate results relying on the cutting plane, the research team decided to use a different method to track the damage within the sample, which is based on tracking the cracks within the sample. This was achieved by activating a crack-monitoring routine, which records and counts the broken bonds, once a bond is broken it is then replaced by a disk to visualize the crack within the sample. Figure 25 illustrates the visualization of broken bonds (cracks) within OT sample.
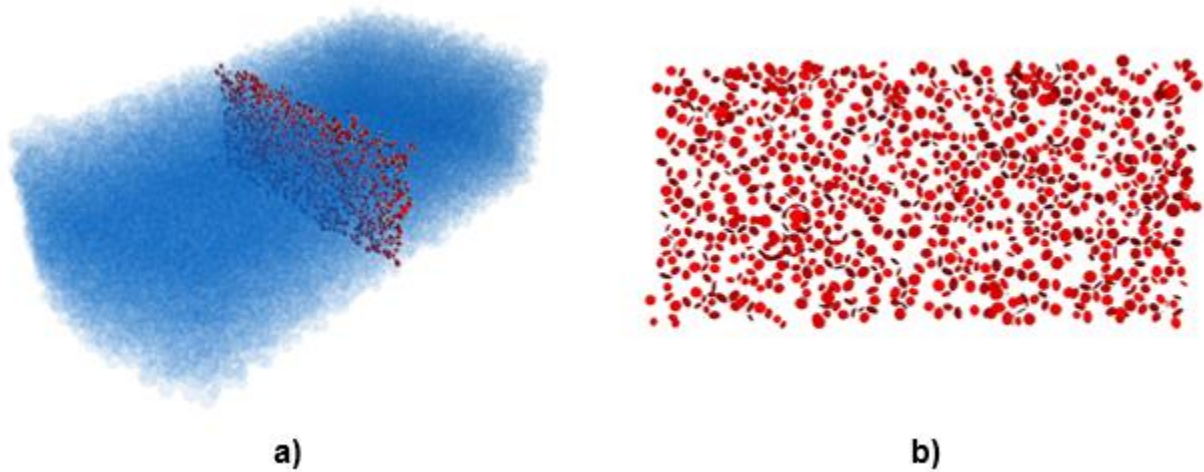
Figure 25. **Overlay Tester Broken Bonds (Red Disks)**

Table 4 summarizes the number of broken bonds for the nine aggregate-mix combinations considered in this study. The unloaded number represent the number of the broken bonds in the OT sample before the simulation start, which is zero as expected, the table also illustrates the number of broken bonds after one loading cycle, two loading cycles, and monotonic loading until complete failure. The results indicated that high percentage of damage occur within the first cycle. For the hard limestone aggregates, the damage percentages after the first cycle were 97.1%, 98.7%, and 98.9% for PFC, CMHB, and Superpave mixes respectively. For the granite, the results were similar; 97.6%, 97.8%, and 97.1% of the damage occurred in the first loading cycle for PFC, CMHB, and Superpave mixes respectively. Finally, the soft lime stone damage percentages were 99.0%, 98.2%, and 95.6% for PFC, CMHB, and Superpave mixes respectively. These results are illustrated visually in Figure 26. Such analysis could be useful if the damage within the first cycle was not as severe as in the cases presented here, with all mixes exhibiting more than 95% of damage in the first cycle. Such high damage indicates that the current OT loading scheme might not be suitable to distinguish between different asphalt mixes.

Table 4. DEM OT Sample Broken Bonds

Aggregate – Mix Type	# of Broken Bonds			
	Unloaded	One Cycle	Two Cycles	Monotonic
Hard Limestone – PFC	0	937	938	965
Hard Limestone – CMHB	0	964	965	977
Hard Limestone – Superpave	0	978	978	989
Granite – PFC	0	985	985	1009
Granite – CMHB	0	971	971	993
Granite – Superpave	0	957	958	986
Soft Limestone – PFC	0	916	916	925
Soft Limestone – CMHB	0	974	975	992
Soft Limestone – Superpave	0	1004	1004	1050
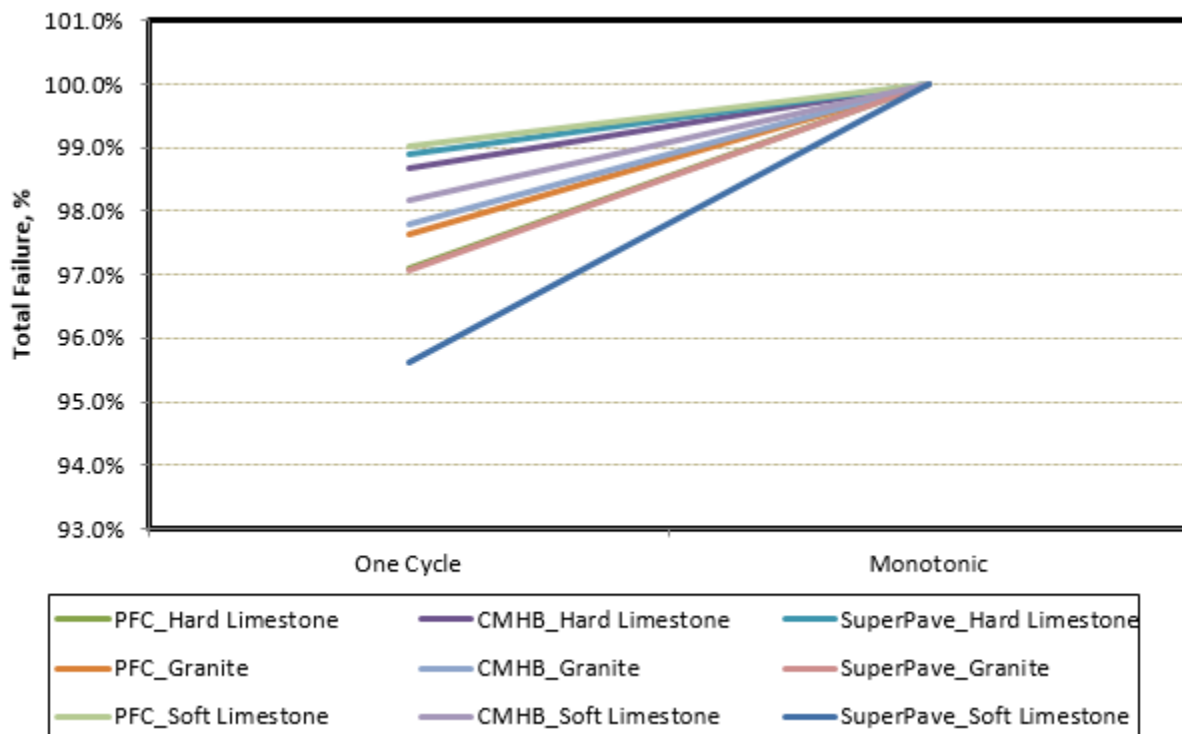
Figure 26. **Percent Failure after One Cycle- Homogenous DEM**
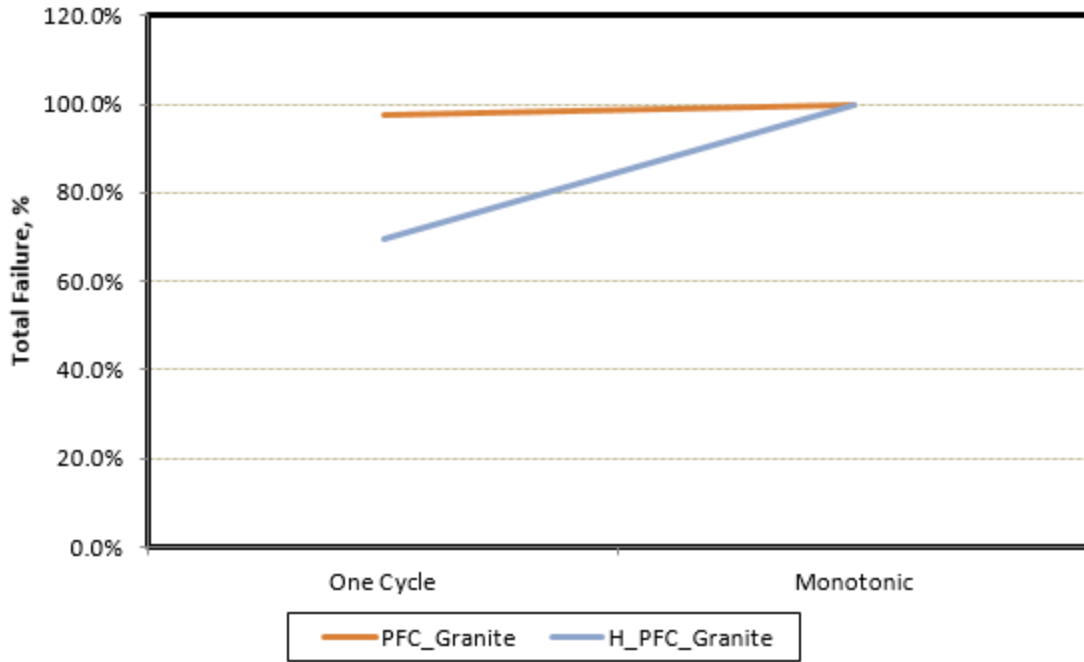
The next analysis in this study focused on heterogeneous OT-DEM simulations. The DEM material parameters from the calibration task of heterogeneous asphalt mixes were used as input for this model. The internal structure was obtained by utilizing the X-ray images of asphalt mixes along with CAD software as described in previous part of

this report. Due to time constraints, only two mixes were considered for this analysis; granite-PFC and hard limestone-PFC. The simulation results are summarized in Table 5. The table also includes the homogenous results for the same cases for comparison. Both mixes exhibited less broken bonds in the first cycle compared to the homogenous cases, additionally, both required more broken bonds to reach failure compared to the homogenous cases. The increase of number of broken bonds to achieve failure is contributed to the inclusion of aggregate particles, which has a higher bond strength, the mastic. Figures 27 and 28 illustrate a comparison between homogenous and heterogonous mixes, for the granite-PFC and hard limestone-PFC mixes, respectively. The granite-PFC mixes had a 69.5% after the first cycle for the heterogonous case compared to 97.6% for the homogenous case, while the hard limestone-PFC mix had a 79.1% damage for the heterogonous case compared to a 99.0% for the homogenous case. These results clearly indicate that the heterogonous OT-DEM model has a much better potential than the homogenous model.

Table 5. DEM OT Sample Broken Bonds (Homogenous vs Heterogeneous)

Aggregate – Mix Type	# of Broken Bonds		
	Unloaded	One Cycle	Monotonic
Granite – PFC	0	985	1009
Granite – PFC (Heterogeneous)	0	892	1284
Soft Limestone – PFC	0	916	925
Soft Limestone – PFC (Heterogeneous)	0	855	1081

Figure 27. Percent Failure after One Cycle- Heterogeneous DEM (PFC Granite Mix)
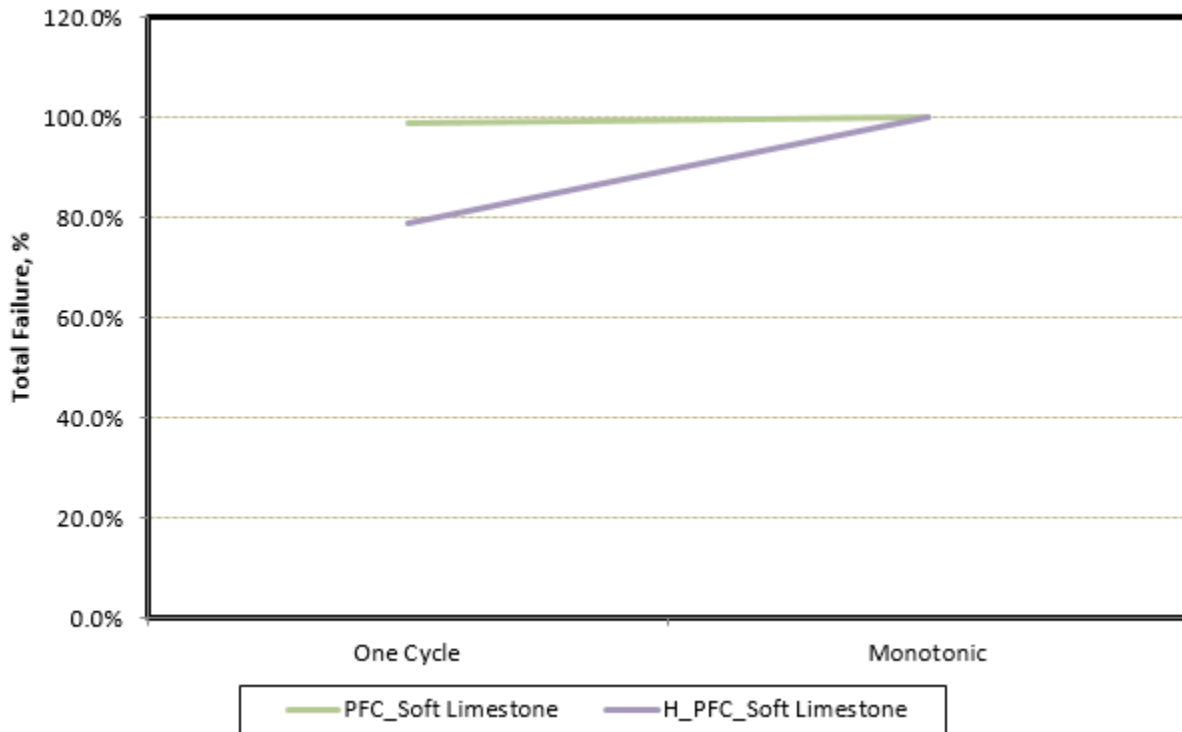
Figure 28. Percent Failure after One Cycle- Heterogeneous DEM (PFC Soft Limestone Mix)

The final analysis of the OT-DEM in this study focused on the investigating the model with rigid wall loading plates excluding the PFC mixes. Table 6 summarizes the number of broken bonds that occurred in the OT samples. The results indicate that all the mixes had similar performance within the first two cycles. Additionally, the same number of broken bonds was observed in the first and second cycle.

Table 6. DEM OT Sample Broken Bonds (Rigid Walls Loading Plates)

Aggregate – Mix Type	# of Broken Bonds			
	Unloaded	One Cycle	Two Cycles	Monotonic
Hard Limestone – CMHB	0	19	19	977
Hard Limestone – Superpave	0	25	25	989
Granite – CMHB	0	14	14	993
Granite – Superpave	0	15	15	986
Soft Limestone – CMHB	0	15	15	992
Soft Limestone – Superpave	0	18	18	1050

SCB Analysis

The final task in this project was to numerically study the SCB test. Three different notch sizes were used: 25.4 mm, 31.75 mm, and 38.1 mm, additionally, three samples were generated for each notch. Heterogeneous SCB-DEM samples were generated by randomly mapping aggregate particles into a homogenous SCB DEM. The mapping process was random in terms of locating the aggregate particles within the sample, but the gradations matched the OT-DEM gradations discussed earlier in this report. Figures 29-31 summarize the 9 samples generated for CMHB, Superpave, and PFC mixes respectively.

Figure 32 shows the strain energy curves for each gradation – aggregate combination per notch. The strain energy decreases as the notch depth increases. CMHB – soft limestone mix stored more strain energy than any other aggregate sources for notch size 25.4 mm. Figure 33 shows the strain energy curves for Superpave mixes. As seen with CMHB samples, the strain energy decreases when the notch depth of the sample increases. Superpave – hard limestone mixes stored less energy than others aggregate sources. Finally, Figure 34 shows the strain curves for PFC mixes. The strain energy decreases as the notch depth increases. PFC – hard limestone mixes failed prematurely under the sample own-weight, due to the weak mastic bond.
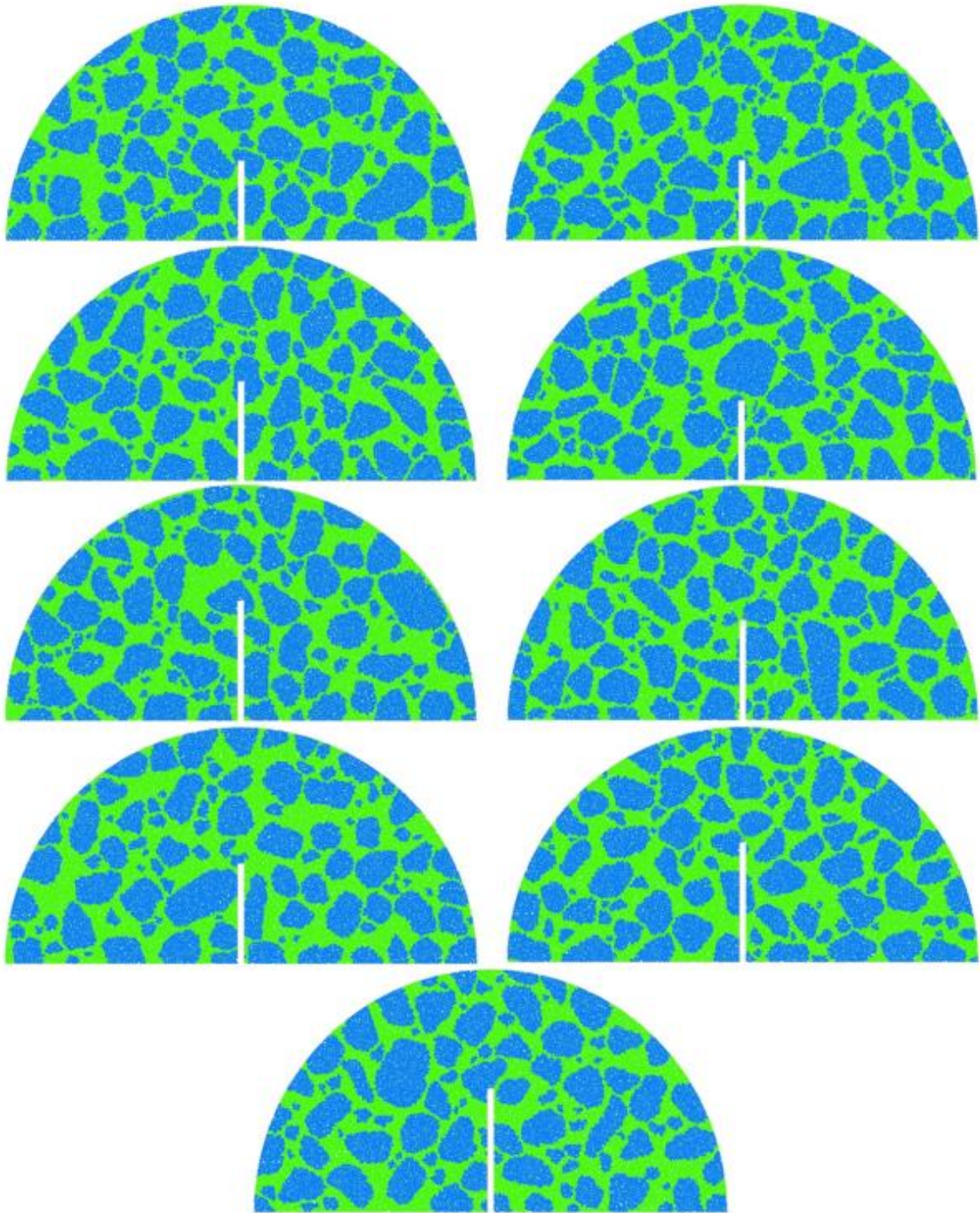
Figure 29. CMHB SCB-DEM Samples
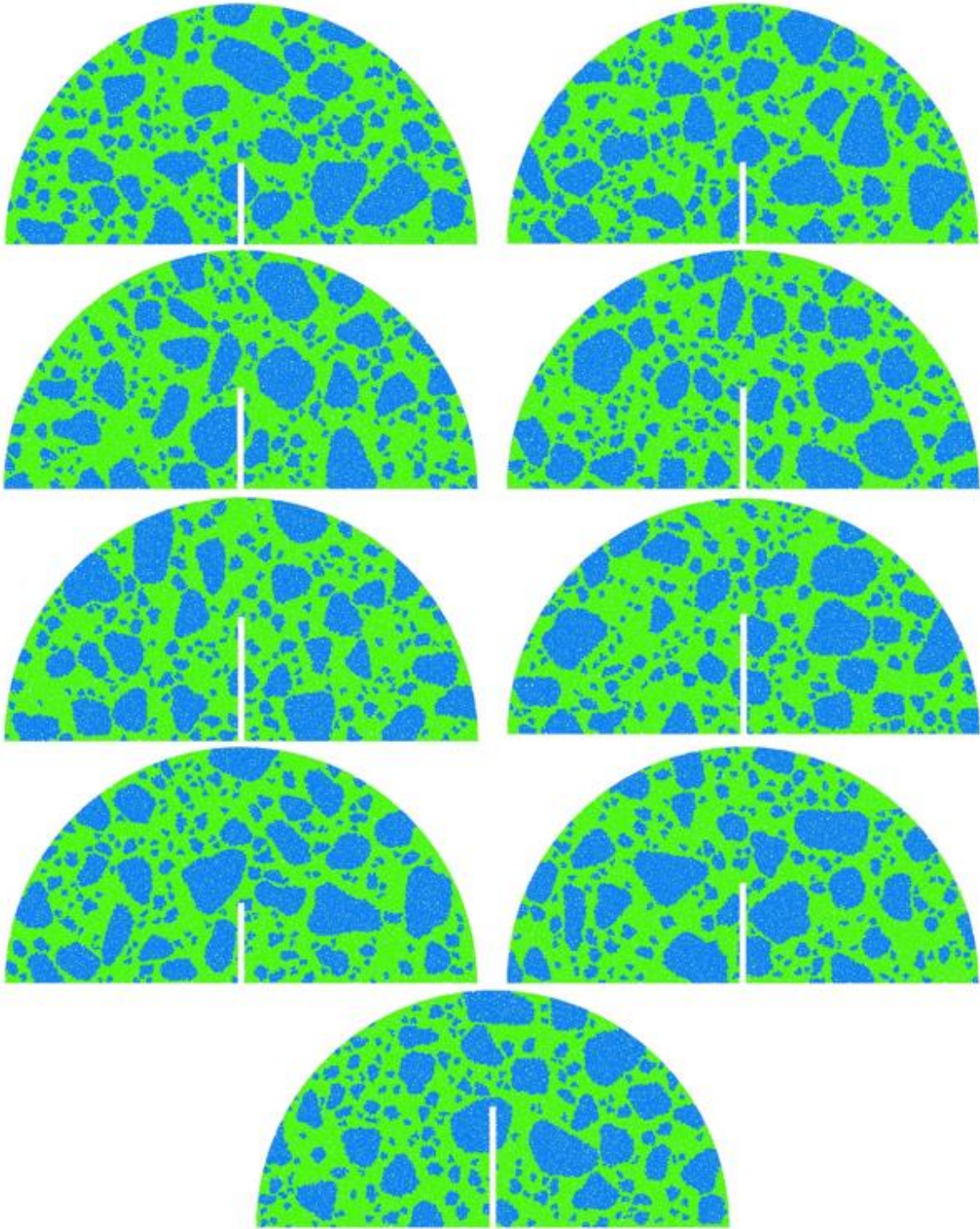
Figure 30. **Superpave SCB-DEM Samples**
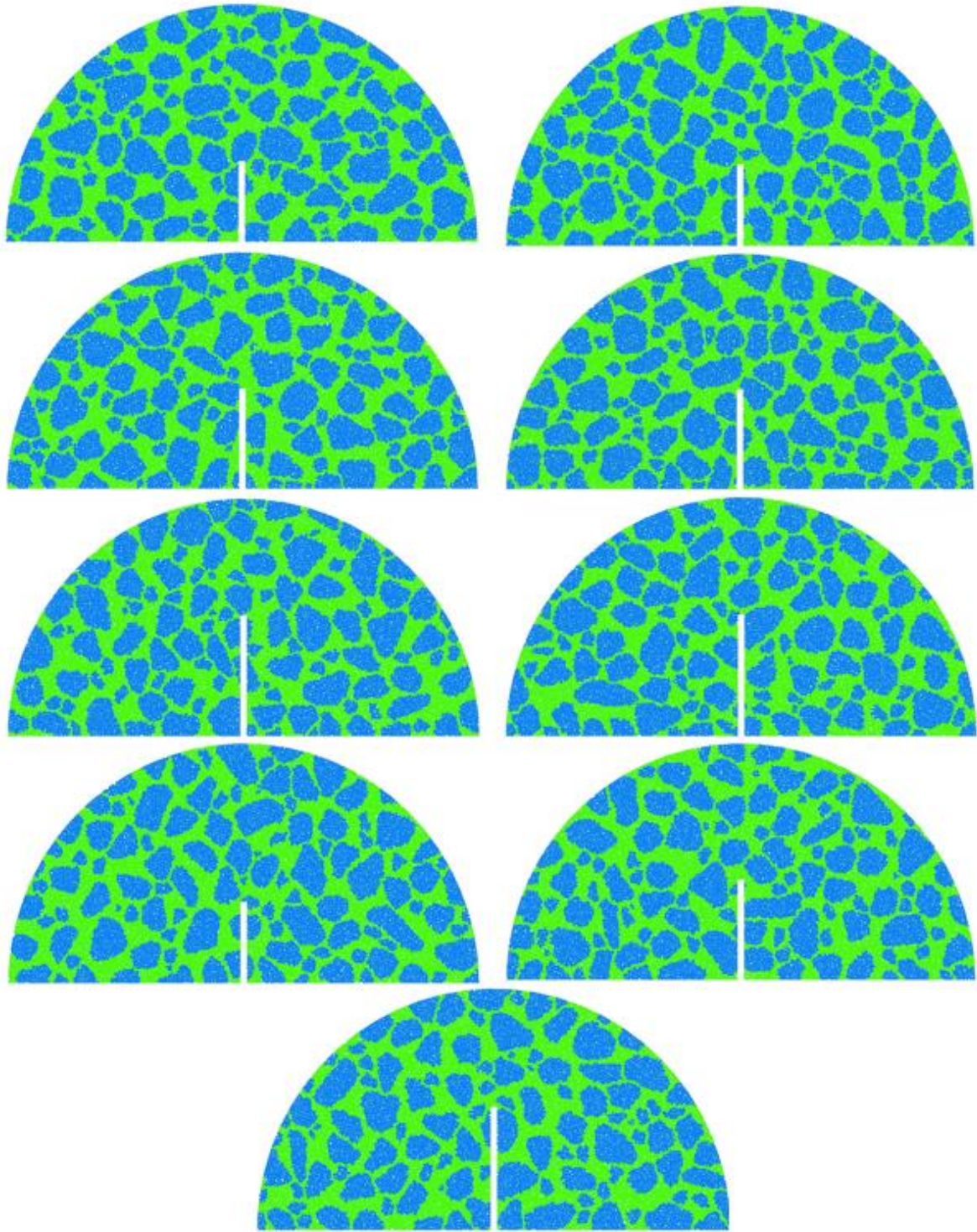
Figure 31. **PFC SCB-DEM Samples**

Table 7. CMHB SCB DEM Maximum Load

Granite	Max Force (N)		
Notch (mm)	1	2	3
25.4	267	267	392
31.8	238	260	248
38.1	154	122	175
Hard Limestone	Max Force (N)		
Notch (mm)	1	2	3
25.4	380	383	536
31.8	327	369	258
38.1	205	183	251
Soft Limestone	Max Force (N)		
Notch (mm)	1	2	3
25.4	442	600	304
31.8	347	278	383
38.1	230	242	197

Table 8. Superpave SCB DEM Maximum Load

Granite	Max Force (N)		
Notch (mm)	1	2	3
25.4	452	595	509
31.8	419	356	326
38.1	243	259	198
Hard Limestone	Max Force (N)		
Notch (mm)	1	2	3
25.4	338	474	386
31.8	327	261	242
38.1	153	209	147
Soft Limestone	Max Force (N)		
Notch (mm)	1	2	3
25.4	525	384	595
31.8	311	381	332
38.1	244	361	215

Table 9. PFC SCB DEM Maximum Load

Granite	Max Force (N)		
Notch (mm)	1	2	3
25.4	150	160	145
31.8	101	102	126
38.1	76	61	68
Hard Limestone	Max Force (N)		
Notch (mm)	1	2	3
25.4	20	16	23
31.8	17	-	-
38.1	-	-	-
Soft Limestone	Max Force (N)		
Notch (mm)	1	2	3
25.4	92	87	74
31.8	48	57	67
38.1	28	27	22
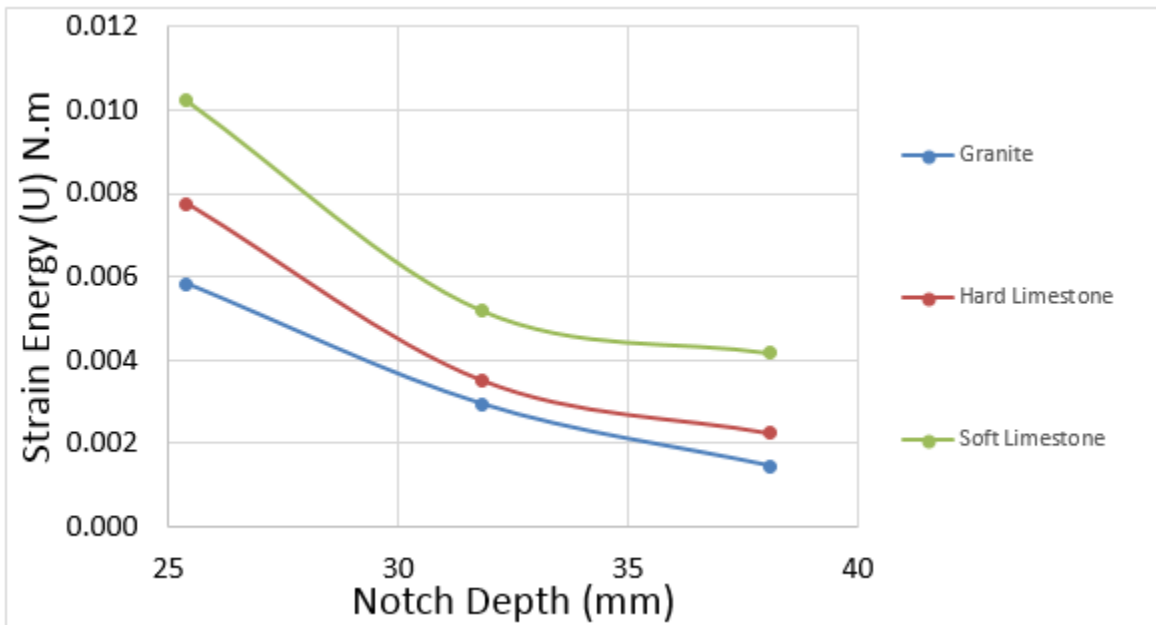
Figure 32. Strain Energy Curves for CMHB mixes
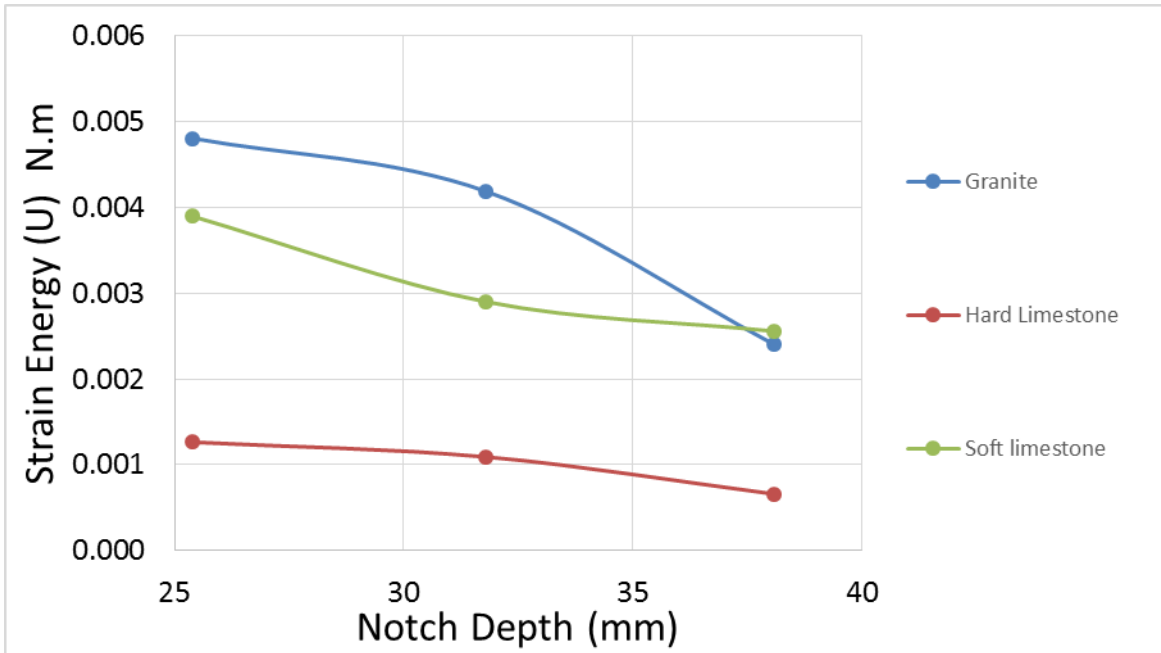
Figure 33. **Strain Energy Curves for Superpave mixes**
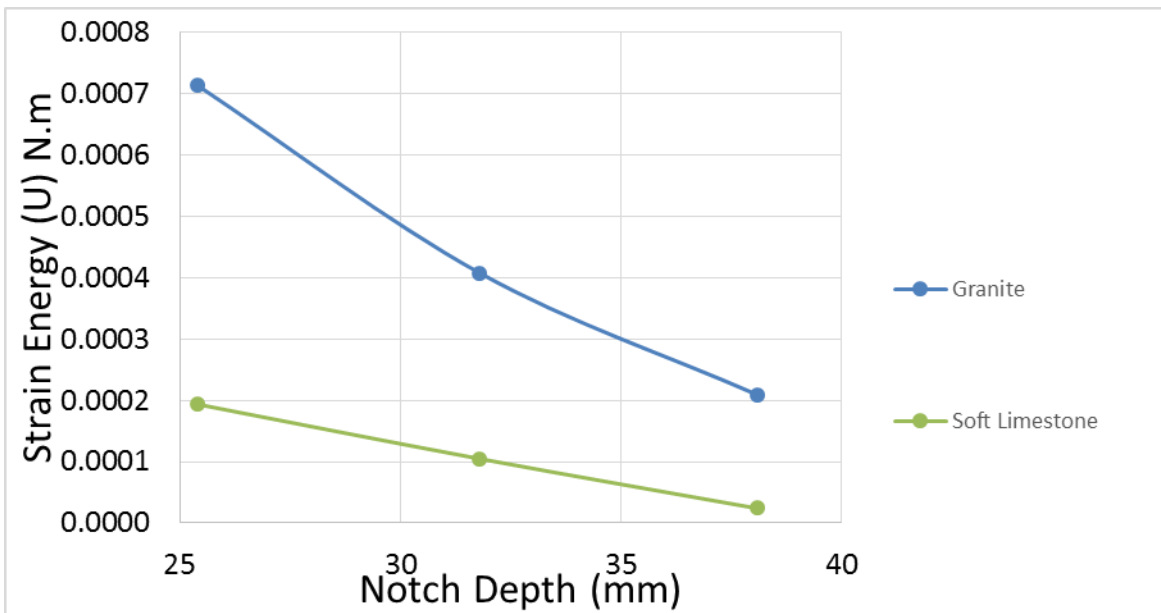
Figure 34. **Strain Energy Curves for PFC mixes**

Discussion, Conclusions, and Recommendations

A numerical model of the OT was developed. The developed model combined DEM with imaging techniques to study asphalt mix crack resistance. Both homogenous and heterogonous model were developed and compared. The development of the OT-DEM model was achieved in four steps. Step 1 focused on developing material-genesis for asphaltic materials, the one phase asphalt material-genesis (homogenous) was based on representing the material with dense-packing of non-uniform circular (2D) or spherical (3D) discrete elements that are bonded at the contact points. Step 2 focused on expanding the model from homogenous to heterogonous. X-ray images were stacked to form the three dimensional representation of the asphalt mixes internal structure (3D aggregate representation). The third step was the addition of the loading plates, three methods were considered: loading plates as rigid walls in DEM, loading plates using DEM particles, and applying the boundary conditions to the bottom of the OT sample. All three methods produced similar results; however, the third method was selected due to its computational time. Finally, the resolution (diameter of the discrete element particles) was studied, and it was concluded that the discrete elements radius range of 1 to 2 mm is sufficient to capture the internal stresses. The materials and mixes selected cover wide range of aggregate gradations, strength, and shape properties, the mixes included were: Superpave-C, CMHB-C, and PFC, while the aggregates were: a hard limestone, soft limestone, and granite. Split tensile testing results for the nine combinations of mixes and aggregates were available in addition to the modulus, compressive strength, and split tensile for the aggregates.

In DEM, which synthesizes macro continuum material behavior from the interactions of micro discrete elements, the input properties usually are not known and can only found by calibration. The calibration process entails setting the micro parameters of the model, such that the simulated test results match material properties measured in similar tests. Thus, in order to obtain proper material properties to run the OT-DEM simulations, calibration was required. The calibration process was performed for homogenous asphalt mixes (split tensile test), rock masses (compressive strength, splitting tensile,

and modulus), and heterogeneous asphalt mixes (splitting tensile). The results for all the calibrations models compared very well with the experimental results.

The DEM material parameters from the calibration task were used as input for the OT-DEM model, the model focused on damage induced in the sample within the first two loading cycle in comparison to the monotonic loading case. Homogenous samples analyses based on the number of active contact bonds in the center of the sample were performed initially, however, due to continuous change of the center of the sample, due to the loading scheme. This led to some inaccurate results, and thus it was decided to use a different method to track the damage within the sample. The method was based on tracking the number of broken bonds (cracks) within OT sample. This analysis indicated that for all the nine combinations of mixes and aggregates, more than 95% damage occurred by the end of the first cycle, which made it impossible to distinguish between asphalt mixes. Heterogeneous OT-DEM simulations for two mixes were performed and compared with the homogenous cases. The results indicated much less damage after the first loading cycle. The granite-PFC mix had 69.5% damage after the first cycle for the heterogonous case compared to 97.6% for the homogenous case, while the hard limestone-PFC mix had 79.1% damage for the heterogonous case compared to a 99.0% for the homogenous case. These results clearly indicate that the heterogonous OT-DEM model has a much better potential than the homogenous model. Further analysis indicated that the use of rigid walls to simulate the loading plates improved the simulation results. Finally, heterogeneous SCB-DEM simulations were conducted for all three mixes with three notch sizes (25.4 mm, 31.75 mm, and 38.1 mm), the numerical simulations were reliable for Superpave and CMHB mixes, the test is not recommended for mixes with high air void content, which manifest itself in this model as very weak mastic (very low bond strength), such as PFC.

Based on the results of the study the following conclusions can be drawn:

- DEM is a viable numerical technique to study crack and fracture within asphalt mixes, it is capable of capturing the viscoelastic behavior and damage can be tracked based on the breakage of the bonds between the model elements.

Additionally, DEM models of splitting tensile test and compressive strength can be successfully used to match laboratory testing results.

- DEM-OT can be successfully simulated with three type of loading conditions: rigid walls, DEM particles loading plates, and applying the boundary conditions to the bottom of the OT sample.

- X-Ray images provide a great mean to develop heterogeneous DEM-OT, however, the process of converting the images to a 3D model is cumbersome, and time consuming. Automating such method would result in less accurate representation of the aggregate shape and size and is not recommended.

- DEM model resolution could affect the accuracy of results, thus, it's very important to conduct a sensitivity analysis to obtain acceptable basic results.

- DEM-OT test is best analyzed by tracking the number of broken bonds rather than attempting to track the active bonds in the center of the sample. Additionally, the numerical simulations are more reliable and meaningful when heterogeneous sample is considered rather than homogeneous one.

- OT-DEM simulation with rigid wall loading plates provided more realistic results and is recommended for future studies.
- SCB-DEM can be successfully simulated and virtual samples can be generated to match typical asphalt mix gradations.

References

1. Abbas, A., Masad, E., Papagiannakis, T., and Harman, T. (2007). "Micromechanical modeling of the viscoelastic behavior of asphalt mixtures using the discrete-element method." International Journal of Geomechanics ASCE, 7(2), 131-139.

2. Abbas, A., Masad, E., Papagiannakis, T., and Shenoy, A. (2005). "Modelling asphalt mastic stiffness using discrete element analysis and micromechanics-based models." International Journal of Pavement Engineering, 6(2), 137-146.

3. Alvarado et al., 2007 Alvarado, Cesar., Mahmoud, Enad., Abdallah, Imad., Masad, Eyad., Nazarian, Soheil., Langford, Richard., Tandon, Vivek., and Button, Joe. (2007). "Feasibility of quantifying the role of coarse aggregate strength on resistance to load in HMA." TxDOT Project No. 0-5268 and Research Report No. 0-5268.

4. Bennert, T. (2009). "Lab Overlay Testers for Characterizing HMA Crack Resistance." 2009 Northeast Asphalt User Producer Group, South Portland, Maine, October 7–8, 2009.

5. Bennert, T. and Dongré, R. (2010). "A Back Calculation Method to Determine 'Effective' Asphalt Binder Properties of RAP Mixtures." Transportation Research Board.

6. Bennert, T., Ali, M., and Sauber, R. (2011). "Influence of Production Temperature and Aggregate Moisture Content on the Performance of Warm Mix Asphalt (WMA)." TRB, Paper Submitted for Presentation and Publication to the 90th Annual Meeting of the Transportation Research Board.

7. Bennert, T., Worden, M., and Turo, M. (2009). "Field and Laboratory Forensic Analysis of Reflective Cracking on Massachusetts Interstate 495." Transportation Research Board

8. Cai, W., McDowell, G., and Airey, G. (2013). "Discrete element modelling of uniaxial constant strain rate tests on asphalt mixtures" Granular Matter, 15(2), 163-174.

9. Cai, W., McDowell, G., and Airey, G. (2014) "Discrete element visco-elastic modelling of a realistic graded asphalt mixture" Soils and Foundations, 54(1), 12-22.

10. Collop, A., McDowell, G., and Lee, Y. (2007), "On the use of discrete element modelling to simulate the viscoelastic deformation behaviour of an idealized asphalt mixture". Geomechanics and Geoengineering Vol. 2, Iss. 2.

11. Cundall, P. A. (1971). "A computer model for simulating progressive large scale movements in blocky rock systems." Proc., Symposium of the International Society of Rock Mechanics, Nancy, France, Vol. 1, Paper No. II-8.

12. Cundall, P. A., and Strack, O. D. L. (1979). "A discrete numerical model for granular assemblies." Geotechnique, 29(1), 47-65.

13. Dai, Q., and You, Z. (2007). "Prediction of creep stiffness of asphalt mixture with micromechanical finite-element and discrete-element models." Journal of Engineering Mechanics ASCE, 133 (2), 163-173.

14. Germann, F. P. and Lytton, R. L., *Methodology for predicting the reflection cracking life of asphalt concrete overlays*, Research report FHWA/TX-79/09+207-5, March 1979.

15. Hajj, E., Sebaaly, P., Porras, J., and Azofeifa, J. (2010). "Reflective Cracking of Flexible Pavements Phase III: Field Verification." Research Report No. 13KJ-1, Nevada Department of Transportation, Research Division, University of Nevada, Reno.

16. Kim, H., Wagoner, M. P., and Buttlar, W. (2008). "Simulation of fracture behavior in asphalt concrete using a heterogeneous cohesive zone discrete element model." Journal of Materials in Civil Engineering ASCE, 20(8), 552-563.

17. Koohi, Y., Luo, R., Lytton, R., and Scullion, T. (2013). "New Methodology to Find the Healing and Fracture Properties of Asphalt Mixes Using Overlay Tester." J. Mater. Civ. Eng., 25(10), 1386–1393.

18. Liu, Y., and You, Z. (2011). "Accelerated Discrete-Element Modeling of Asphalt-Based Materials with the Frequency-Temperature Superposition Principle." Journal of Engineering Mechanics, 137(5), 355-365.

19. Liu, Y., and You, Z. (2011). "Discrete-Element Modeling: Impacts of Aggregate Sphericity, Orientation, and Angularity on Creep Stiffness of Idealized Asphalt Mixtures." Journal of Engineering Mechanics, 137(4), 294-303.

20. Liu, Y., Dai, Q., and You, Z. (2009). "Viscoelastic Model for Discrete Element Simulation of Asphalt Mixtures." J. Eng. Mech., 135(4), 324–333.

21. Mahmoud, E., Masad, E., and Nazarian, S. (2010) "Discrete Element Analysis of the Influence of Aggregate Properties and Internal Structure on Fracture in Asphalt Mixtures," Journal of Materials in Civil Engineering, (ASCE) Vol. 22 No. 1, pp 10-20.

22. Mahmoud, E., Masad, E., Nazarian, S., and Abdallah, I. (2010) "Modeling and Experimental Evaluation of Influence of Aggregate Blending on Asphalt Mixture Strength," Journal of Transportation Research Board, (TRB) Vol. 2180, pp 48-57.

23. Potyondy, D. O., and P. A. Cundall. (2004) "A Bonded-Particle Model for Rock," Int. J. Rock Mech. & Min. Sci., 41(8), 1329-1364.

24. Walubita, L., Abu N. Faruk, Gautam Das, Hossain A. Tanvir, Jun Zhang, and Tom Scullion (2012). "The overlay tester: a sensitivity study to improve repeatability and minimize variability in the test results" Research Report No. FHWA/TX-12/0-6607-1, Texas Transportation Institute, Texas A&M University System, College Station, Texas.

25. Walubita, L., Abu N. Faruk, Yasser Koohi, Rong Luo, Tom Scullion, and Robert L. Lytton (2013). "The Overlay tester (OT): Comparison with Other Crack Test Methods and Recommendations for Surrogate Crack Tests" Research Report No. FHWA/TX-13/0-6607-2, Texas Transportation Institute, Texas A&M University System, College Station, Texas.

26. Wu, J., Collop, A., and McDowell, G. (2011). "Discrete Element Modeling of Constant Strain Rate Compression Tests on Idealized Asphalt Mixture." J. Mater. Civ. Eng. 23, SPECIAL ISSUE: Multiscale and Micromechanical Modeling of Asphalt Mixes, 2-11

27. You, Z., and Buttlar, W. G. (2004). "Discrete element modeling to predict the modulus of asphalt concrete mixtures." Journal of Materials in Civil Engineering ASCE, 16(2), 140-146.

28. You, Z., and Buttlar, W. G. (2005). "Application of discrete element modeling techniques to predict the complex modulus of asphalt—aggregate hollow cylinders subjected to internal pressure." Transportation Research Record 1929, Transportation Research Board, Washington, DC; pp 218–226.

29. You, Z., Liu, Y., and Dai, Q. (2011). "Three-Dimensional Microstructural-Based Discrete Element Viscoelastic Modeling of Creep Compliance Tests for Asphalt Mixtures." J. Mater. Civ. Eng. 23, SPECIAL ISSUE: Multiscale and Micromechanical Modeling of Asphalt Mixes, 79–87.

30. Zhou, F. and Scullion, T. (2005). "Overlay Tester: A Rapid Performance Related Crack Resistance Test." Research Report No. FHWA/TX-04/0-4467-2, Texas Transportation Institute, Texas A&M University System, College Station, Texas.